THE REPUBLIC OF TURKEY

BAHCESEHIR UNIVERSITY

UNDERWATER ELECTRO-OPTIC INTERCOM SYSTEM DESIGN

Master Thesis

KAAN ALPER

ISTANBUL, 2018

THE REPUBLIC OF TURKEY
BAHCESEHIR UNIVERSITY

GRADUATE SCHOOL OF NATURAL AND APPLIED SCIENCES
ELECTRICAL AND ELECTRONICS ENGINEERING

UNDERWATER ELECTRO-OPTIC INTERCOM SYSTEM DESIGN

Master Thesis

KAAN ALPER

Thesis Advisor: Associate Professor Dr. Sarper ÖZHARAR

ISTANBUL, 2018

THE REPUBLIC OF TURKEY
BAHCESEHIR UNIVERSITY

GRADUATE SCHOOL OF NATURAL AND APPLIED SCIENCES
ELECTRICAL AND ELECTRONICS ENGINEERING

Name of the thesis: Underwater Electro-Optic Intercom System Design
Name/Last Name of the Student: Kaan ALPER
Date of the Defense of Thesis: 08.01.2018

The thesis has been approved by the Graduate School of Natural and Applied Sciences.

Prof. Dr. Nafiz ARICA
Graduate School Director

I certify that this thesis meets all the requirements as a thesis for the degree of Master of Arts.

Asst. Prof. Cavit Fatih KÜÇÜKTEZCAN
Program Coordinator

This is to certify that we have read this thesis and we find it fully adequate in scope, quality and content, as a thesis for the degree of Master of Arts.

Examining Comittee Members	Signature
Thesis Supervisor Assoc. Prof. Sarper ÖZHARAR	_____
Member Asst. Prof. Ömer POLAT	_____
Member Prof. Dr. Alphan SENNAROĞLU	_____

ACKNOWLEDGEMENT

Thanks to…

My supervisor Assoc. Prof. Sarper ÖZHARAR for guiding and supporting me over the years, for sharing his valuable knowledge with me and for his understanding.

My thesis committee members for all their guidance through my thesis process.

My director Selçuk ÖZYURT for his understanding and his helps through solving complicated electronic problems.

My family for being patient with my perpetual studentship, they have never lost their faith in me.

My wife Dr. Ezgi Ceren Dallı ALPER for her mental and motivational support while she was on duty far from home in Şırnak. She is my inspiration and motivation for continuing to improve my knowledge and move my career forward.

Finally, I would like to thank and dedicate my thesis to my grandfather and all other family members that passed away. He was the kindest and the most diligent person I have ever seen. Although it has been years since you have passed, I still keep your suggestions with me, every day.

Istanbul, 2018 Kaan ALPER

ABSTRACT

UNDERWATER ELECTRO-OPTIC INTERCOM SYSTEM DESIGN

Kaan ALPER

Electrical and Electronics Engineering

Thesis Advisor: Associate Professor Dr. Sarper Özharar

January 2018, 71 pages

The underwater optical communication is getting more popular day by day. About 71 % of the Earth's surface is covered with water and 96,5 % of this covered area is the oceans. During the past thousand years, human have never stopped exploring the oceans. Most of the comprehensive ocean explorations made underwater world and it became a great interest to the scientific, industrial and military societies. Underwater communication makes the underwater explorations possible. Bidirectional and secure underwater communication is a very challenging task even with nowadays technology, because the methods for wireless communication in air, do not work in water. In this thesis, Radio Frequency, acoustic and optical communication methods for underwater environment are inspected by comparing advantages and disadvantages of the methods. In addition to this, one transmitter and one receiver of underwater optical communication electronic system and one laryngophone system prototype is designed and constructed. The directional optical communication between one transmitter and one receiver has been successfully demonstrated on the field and error free audio communication has been successfully accomplished at a distance of 60 meters.

Keywords: underwater, visible optical communication, wireless optical communication.

ÖZET

SUALTI ELEKTRO OPTIK İNTERKOM SİSTEMİ TASARIMI

Kaan ALPER

Elektrik ve Elektronik Mühendisliği

Tez Danışman: Doç. Dr. Sarper Özharar

Ocak 2017, 71 sayfa

Sualtı optik iletişimi her geçen gün daha popüler hale gelmektedir. Dünya yüzeyinin %71'i su ile kaplı olduğu gibi bu %71' in %96,5'ini okyanuslar oluşturmaktadır. Geçen bin yıl boyunca, insanoğlu okyanusları keşfetmeyi hiç bırakmamıştır. Kapsamlı okyanus araştırmalarının çoğu su altı dünyasında yapılmış ve bilimsel, endüstriyel ve askeri sektörler tarafından büyük ilgi görmüştür. Sualtı keşifleri ancak ve ancak sualtı haberleşmesi ile mümkün kılınır. Çift yönlü ve güvenli sualtı iletişimi, havadaki kablosuz iletişim yöntemleri suda çalışmadığından ötürü, günümüz teknolojisiyle bile çok zordur. Bu tez çalışmasında, sualtı ortamında radyo frekansı, akustik ve optik iletişim yöntemleri, ilgili yöntemlerin avantaj ve dezavantajları karşılaştırılarak incelenmiştir. Buna ek olarak, bir verici ve bir alıcı sualtı optik iletişim sistemi elektronik tasarımı ve üretimiyle bir adet gırtlak mikrofonu prototipi yapılmıştır. Bir verici ve bir alıcı arasında yönlü optik iletişim başarılı bir şekilde gerçekleştirilmiş olup, hatasız sesli iletişim 60 metrelik bir mesafede gerçekleştirilmiştir.

Anahtar Kelimeler: Sualtı, görünür ışık optik iletişim, kablosuz optik iletişim.

CONTENTS

TABLES

FIGURES

ABBREVIATONS

A	:	Ampere
ARM	:	Acorn RISC Machines
CW	:	Clockwise
CPU	:	Central Processing Unit
D	:	Distance
dB	:	Decibel
DC	:	Direct Current
E	:	Efficiency
ELF	:	Extremely Low Frequency
EM	:	Electro Magnetic
EMI	:	Electro Magnetic Immunity
FPGA	:	Field Programmable Gate Array
g	:	Gram
Hz	:	Hertz
IR	:	Infrared
kg	:	Kilogram
KHz	:	Kilohertz
Km	:	Kilometer
LED	:	Light Emitting Diodes
m	:	Meter
MHz	:	Megahertz
ml	:	Milliliter
mm	:	Millimeter
mV	:	Millivolt
mW	:	Milliwatt
nF	:	Nanofarad
nm	:	Nanometer

OWC	:	Optical Wireless Communication
PCB	:	Printed Circuit Board
PFM	:	Pulse Frequency Modulation
PLL	:	Phase Locked Loop
R	:	Resistance
RF	:	Radio Frequency
RSTC	:	Recreational Scuba Training Council
S	:	Siemens
SLF	:	Super Low Frequency
UOWC:		Underwater Optical Wireless Communication
US	:	United States
V	:	Voltage
VLF	:	Very Low Frequency
W	:	Watt

SYMBOLS

Absorption Coefficient	:	$a(\lambda)$
Absorption Coefficient of Fluvic Acid	:	a_f^0
Absorption Coefficient of Humic Acid	:	a_h^0
Absorption of Pure Water	:	a_w
Attenuation	:	α
Attenuation Coefficient	:	$c(\lambda)$
Backscattering	:	$b_B(\lambda)$
Concentration of Chlorophyll-a	:	C_c^0
Concentration of Fluvic Acid	:	C_f
Concentration of Humic Acid	:	C_h
Concentration of Large Particles	:	C_l
Concentration of Small Particles	:	C_s
Conductance	:	G
Conductivity	:	σ
Cubic Meter	:	m^3
Current	:	I
Depth	:	h
Diameter	:	Ø
Diffuse Attenuation Coefficient	:	$K_d(\lambda)$
Direct Current Voltage	:	V_{dc}
Exponential Coefficient of the Fluvic Acid	:	k_f
Exponential Coefficient of the Humic Acid	:	k_h
Fluid Density	:	ρ
Frequency	:	f
Input Voltage	:	V_{in}
Logarithmic Voltage Ratio	:	dBV
Micro Farad	:	µF

Micro Volt	:	μV
Micro	:	μ
Ohm	:	Ω
Omega	:	ʊ
Output Voltage	:	V_{out}
Optical Power	:	I
Particle Velocity	:	u
Peak to Peak Voltage	:	V_{pp}
Pi	:	π
Power	:	P
Pressure	:	p
Probability of Backscattering by large particles	:	$b_l(\lambda)$
Probability of Backscattering by small particles	:	$b_s(\lambda)$
Pure Water Scattering	:	$b_w(\lambda)$
Refractive Index of Water	:	n
Salinity	:	s
Scattering	:	$b(\lambda)$
Specific Scattering Coefficients for large particles	:	$b_l^0(\lambda)$
Speed of light in free space	:	c
Speed of light in water	:	V_{water}
Square Meter	:	m^2
Transmitted Power	:	I_0
Volt	:	V
Wavelength	:	λ

1. INTRODUCTION

Communication has a really important role in society. Communication is derived from the latin word “communis”, means “make common”. Therefore, Communication means “to share” thoughts, ideas, messages and information by the way of speech, writing or signals. Through the communication, the world is safer, more efficient and enjoyable. However, communication has not accomplished the same impact under the water, although it is crucial for diver’s life.

For underwater communication, several methods and technologies are used by divers. These methods are using underwater writing slates, sign languages and electronic communicators (Oceanreef, 2010). Using hand sign languages are considered the most convenient and reliable way to communicate under the water (Oceanreef, 2010). Some of the most common hand sign languages are shown in Table 1.1.

Table 1.1: Most Common Hand Sign Languages by RSTC (Recreational Scuba Training Council)

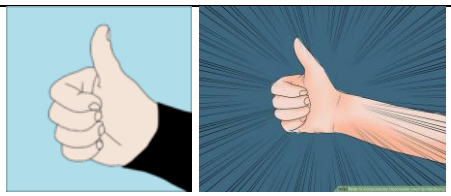	Ascend, or I am going up (RSTC, 2005) (wikiHow, 2017).
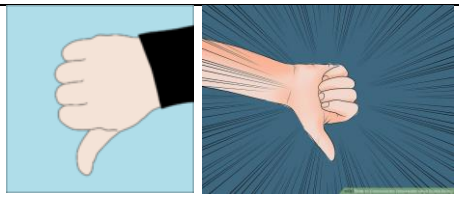	Descend, or I am going down (RSTC, 2005, wikiHow, 2017).
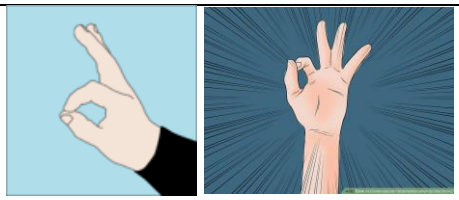	Are you Ok? Or I am Ok! (RSTC, 2005, wikiHow, 2017).

There are varieties of electronic communicators, like using hydrophones, hard wire cables, radio frequency or acoustic. Hydrophones are waterproof sound transceivers

that produce audible sound and listen underwater, however there are limited use of hydrophones for classic diver communications, because it requires considerable power to reach required distances. The most popular communication method is hard wire communication. It is used between surface and divers, sound gathered by microphone and speaker integrated full-face masks and it has the best audio quality but on the other hand, it reduces mobility of divers and limits divers range. It also provides half and full duplex communications, however it is only used by deep divers, underwater workers and divers who need to be connected to surface for further supply needs (Oceanreef, 2010). Also, it requires expensive equipment, since divers are using different technologies to communicate wirelessly such as RF (Radio Frequency) and acoustic.

Radio Frequency based underwater communications held on mostly VLF (Very Low Frequency) and ELF (Extremely Low Frequency) radio waves. In both frequencies, underwater RF communication system requires large sized antennas and it consumes high energy when it is compared with other methods, because RF signals experience high losses when propagating through the water (Waite, 2002). On acoustic based underwater communication, sound is modulated on higher frequencies that human ears cannot detect. The speed of the acoustic waves in water is much greater than the acoustic waves in the air (Oceanreef, 2010). Due to this property of sound in the water, ultrasonic communicators are a part of underwater noise pollution that can affect marine organisms (Peng et al., 2015). Both technologies are one-time & one-way communication which is called half duplex communication, have low frequency signals that can carry low data rates due to limited physical characteristics and these signals are transmitted omni-directional, it means they can be intercepted or jammed by third parties. There is more energy efficient, more secure and more reliable way to communicate under the water: Optical Wireless Communication.

Light has been around for many millions of years. It has created life; it has created all the stuff needed for life. For many years, light has been used for making fire, for illumination, for healing, for heating, for signaling, for communication et cetera. Optical wireless communication exists for many years in form of beacon fires and smoke signals to convey a message and it can be found in almost all cultures.

The recent advancement in technology has gained significant pace after the invention of lasers and LEDs (light-emitting-diodes). Technology has been improving for the last few decades. Improvement in technology has effects on many areas such as everyday lives, social structures and communication. Since humans are limited in their ability to communicate underwater, as it is mentioned above, a solution is brought forth by creating a short range Underwater Optical Wireless Communication (UOWC) system based on LED, to overcome many of the obstacles presented in underwater communication. In this paper, a detailed report is given why and how a short range underwater optical wireless communication system is designed.

A brief introduction of the problem is given on this chapter. The following chapters will firstly be presenting the state of the art on underwater communication methods by indicating physical properties of the water. Secondly, it will be focused on the design and development of the short range UOWC by defining materials and by describing methods that will be used. Third, a detailed electronical and mechanical design will be given. Finally, electro-mechanical system integration will be explained and the results will be discussed.

2. STATE of the ART

In this chapter, historical background of underwater communication and all the necessary scientific works are presented, including methods, related theoretical backgrounds and all the advantages & disadvantages for each approach.

2.1 BACKGROUND

Underwater communication has a long history starting with the knowledge of sound propagating under the water. “If you cause your ship to stop, and place the head of a long tube in the water, and place the outer extremity to your ear, you will hear ships at a great distance from you.” Written in 1490 by Leonardo da Vinci (Benvenuto et al., 2011). But it was not widespread till the concept of submarine would be heard during World War I, therefore, research into underwater sound measurement systems became a necessity. In 1915, two physicists; Ernest Rutherford and Paul Langevin independently created a device for detecting the noise emitted from moving submarines by using piezoelectricity (Katzir, 2012). In 1945, the first underwater voice communication was performed by the Naval Underwater Sound Laboratory (Quazi and Konrad, 1982).

Free Space Optical Communication or Optical Wireless Communication (OWC) is an ancient technology that causes a transmission of an information carrying optical radiation, from one point to another, through a medium. Ancient Greeks and Romans used fire beacons for signaling, by 800 BC (Ghassemlooy et al., 2013). In 1880, first optical voice communication was performed by Alexander Graham Bell, with a device called Photophone (Hospitalier, 1882). Graham Bell constructed a system that modulated the sun radiation by his voice signal and transmitted to a distance of 200 meters.

Figure 2.1: Demonstration of Alexander Graham Bell's Photophone.

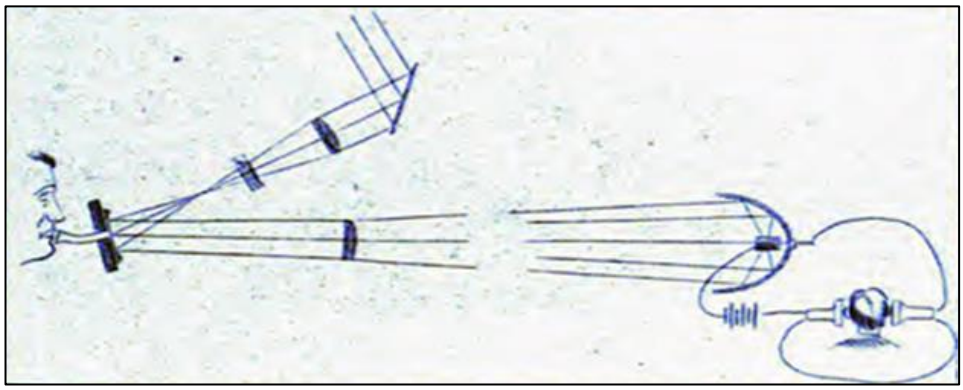

Source: BELL, A. G. 1880. On the Production and Reproduction of Sound by Light. American Journal of Science, 20, 305-324.

Vibrations caused by the voice modulated the reflected sun radiation by a movable mirror, projected and transformed back into voice at the receiver. Photophone never became a commercial product due to its complex mechanical design and the intermittent nature of the sunlight, but it was attracted the interest of the military and high-pressure arc lamps were used to transmit voice in the tactical field (Uysal et al., 2016).

The following century, fiber optic and radio frequency communications improved rapidly and it started to dominate the telecommunication market. But in 1960, the invention of laser is accepted as a substantial milestone of wireless optical communication history (Beleffi, 2010). In 90s the idea of bidirectional ground-satellite laser communications became popular, and after the year 2000, research on the Free Space Optical (FSO) technologies expended all over the world, it is started to be seen in civil and military FSO applications more often (Beleffi, 2010).

Due to improvements in technology, underwater free space optical communication systems have become more popular in recent years with the invention of reliable, low cost light sources such as Light Emitting Diodes (LED) and diode lasers. In 1963, right after 3 years from invention of laser, Seibert Duntley proposed that light with wavelengths of 450nm to 550nm have relatively low attenuation property while passing through seawater (Duntley, 1963) and this property was experimentally proven by G. D. Gilbert and his friends in 1966 (Gilbert et al., 1966). The most comprehensive work has been done by N. G. Jerlov (Jerlov, 1976) and Mobley (Mobley, 1994). The biggest challenges are the attenuation and the scattering properties of water medium and it makes UOWC a very

challenging task. Due to the conducting and dynamically changing sea environment, most common used ways to communicate in air, do not work in water.

2.2 UNDERWATER WIRELESS COMMUNICATION (UWC) TYPES

There are three different types of communication on in the aquatic environment. These are Radio Frequency, Acoustic and Optic.

2.2.1 RADIO FREQUENCY (RF) COMMUNICATION

The term of "wireless" is generally used to describe RF technologies due to common usage of RF devices around the world. Radio Frequencies are consisted of electromagnetic waves and these are a form of radiant energy released by electromagnetic processes (Holt et al., 2010). Electromagnetic spectrum is formed by the frequency range of electromagnetic waves. The wavelength λ is reciprocally related to its frequency *f* by the relationship:

$$\lambda = \frac{c}{f} \qquad \textbf{2.1}$$

where c is the speed of light in free-space with $c \approx 3 \times 10^8 \ {}^{m}/_{s}$.

Table 2.1: The radio spectrum bands.

Frequency	Wavelength	Designation	Acronym.	IEEE band
3-30 Hz	$10^5 - 10^4$ km	Extremely Low Frequency	ELF	-
30-300 Hz	$10^4 - 10^3$ km	Super Low Frequency	SLF	-
300-3000 Hz	$10^3 - 100$ km	Ultra Low Frequency	ULF	-
3-30 kHz	100 – 10 km	Very Low Frequency	VLF	-
30-300 kHz	10 – 1 km	Low Frequency	LF	-

300kHz–3MHz	1 km – 100 m	Medium Frequency	MF	MF
3-30 MHz	100 – 10 m	High Frequency	HF	HF
30-300 MHz	10 – 1 m	Very High Frequency	VHF	VHF
300MHz–3GHz	1 m – 10 cm	Ultra High Frequency	UHF	UHF, L, S
3-30 GHz	10 – 1 cm	Super High Frequency	SHF	S,C,X,Ku,K,Ka
30 – 300 GHz	1 cm – 1 mm	Extremely High Frequency	EHF	Ka, V, W, mm

Source: IEEE 2009. IEEE Standard Letter Designations for Radar-Frequency Bands. In: SOCIETY, I. A. E. S. (ed.) IEEE Std 521-2002. New York: IEEE.

The RF is a very popular choice to communicate via wireless in terrestrial communications. However, underwater electromagnetic communications have been also very popular since the early days of radio (Lindsay, 1853, Lindsay, 1854, Lindsay, 1860) and had drawn great attention during 1960's (Siegel and King, 1973). During this era, terrestrial radio frequency type communication was delivered by Morse Code or full band analogue voice communications over long distances. Researche aimed at performing these types of communications in the aquatic environment. Actually, ELF and SLF submarine communication is believed to be the only successfully performed electromagnetic operation under the water (U.S.Navy, 2003). According to report, US system and Russian system were respectively operating at 76 Hz and 82 Hz. Both systems were capable of transmitting a few characters per minute across the world. It was also capable of performing a one-way "bell ring" to call an individual submarine to the surface for terrestrial radio communication.

There are many restricting factors when performing RF communication in water. EM waves are severally attenuated in the aquatic environment; besides, they have different behavior in freshwater and seawater. Water is an insulator in its pure form, whereas, in nature, it contains dissolved salts and other compounds that make it a good partial conductor. Conductivity (σ) depends on both salinity and temperature of water. Sea water has a high conductivity when it is compared with fresh water, due to its high salt content

(Butler, 1987). High conductivity leads to strong attenuation of electromagnetic waves that are passing through water. A conducting element is defined as the following equation;

$$G=\frac{I}{V}=\frac{1}{R} \qquad \textbf{2.2}$$

Where G is conductance, I is electrical current, V is electrical voltage and R is the electric resistance. The unit of conductance is Siemens and is shown by S and the rest;

$$S=\frac{1}{\Omega}=\Omega^{-1}=\frac{A}{V} \qquad \textbf{2.3}$$

Where Ω is the ohm, A is the ampere and V is the volt. Formerly, mho was used instead of Siemens. It is the reciprocal of the ohm, it is also backwards spelling of ohm and is shown upside down Greek letter omega; ℧.

In Figure 2.2 underwater RF attenuation versus frequency is shown based on Lloyd Butler's work done in 1987. They took the seawater sample from the Red Sea and the freshwater sample from Adelaide. The Red Sea has high salt content, its conductivity varying from 2 S/min the cold region, to 8 S/min the warm region and average conductivity of the sea is about 4 S/m. The Adelaide water has a lower conductivity around 0,0546 S/m.

Figure 2.2: Underwater RF Attenuation versus Frequency

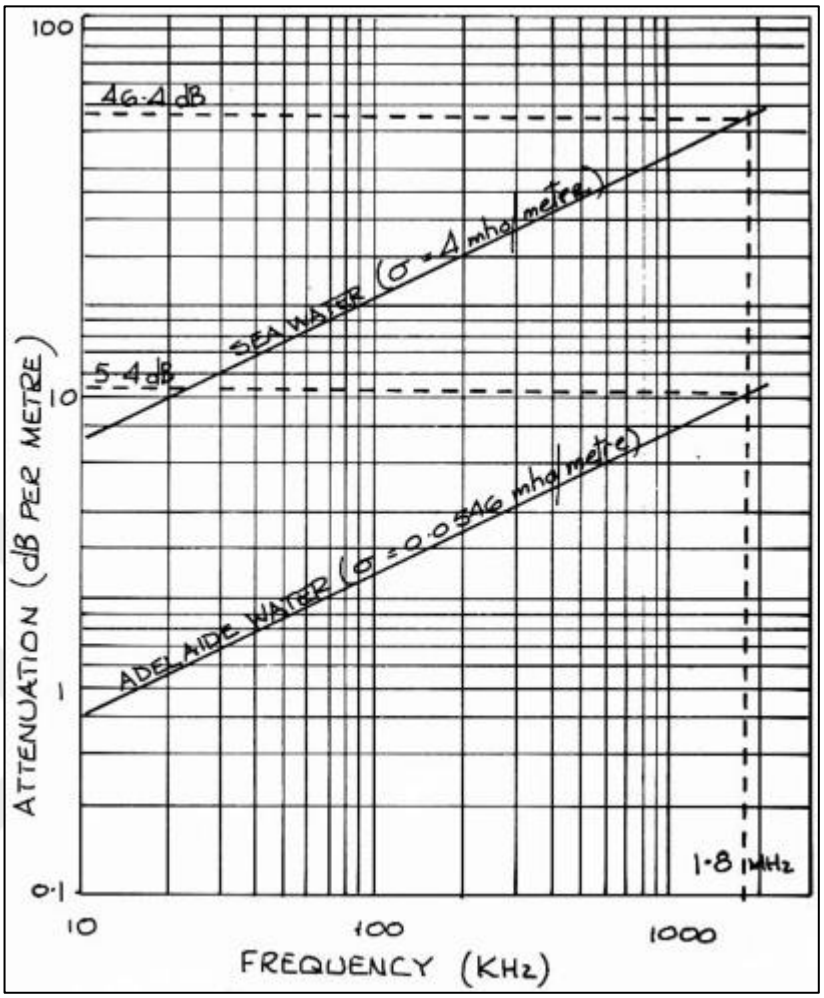

Source: BUTLER, L. 1987. Underwater Radio Communication. Amateur Radio. Melbourne: Wireless Institute of Australia.

The attenuation of the radio wave in the aquatic environment is calculated from the following equation;

$$\alpha=0{,}0173\times\sqrt{(f\times\sigma)} \qquad \textbf{2.4}$$

Where the is attenuation is α, f is the frequency and σ is conductivity. The unit of attenuation is $^{dB}/_{m}$, frequency and conductivity are respectively *Hz* and $^{S}/_{m}$. From the equation **α**=0,0173×$\sqrt{(f\times\sigma)}$ 2.4, a frequency of 62.5 kHz will be attenuating 1,01 $^{dB}/_{m}$ in fresh water, hence it is attenuating 8,65 $^{dB}/_{m}$ in seawater with average salinity. But for a frequency of 62,5 Hz will be attenuating 0,032 $^{dB}/_{m}$ in fresh water and it is attenuating 0,273 $^{dB}/_{m}$ in seawater with average salinity. As it is easily seen that lower frequencies are less attenuating than higher frequencies.

The wavelength propagation is also different in water medium. It is calculated by the following equation:

$$\lambda = 1000 \times \sqrt{10/(f \times \sigma)} \qquad \textbf{2.5}$$

Where λ is the wavelength in meters, f is the frequency in Hz and σ is the conductivity in S/m. To reveal the correlation between the seawater and the fresh water Adelaide, the wavelength in space is taken as reference. From the equation $\lambda = 1000 \times \sqrt{10/(f \times \sigma)}$ ***2.5*** $\lambda = 1000 \times \sqrt{10/(f \times \sigma)}$ ***2.5***, the wavelength of a frequency of 62.5 kHz will be in 54,13 meters in fresh water, 6,32 meters in seawater but it is normally 4,8 km for wavelength in space from equation $\lambda = \frac{c}{f}$ ***2.1***. The difference can also be seen on Figure 2.3.

Figure 2.3: Wavelength versus Frequency.

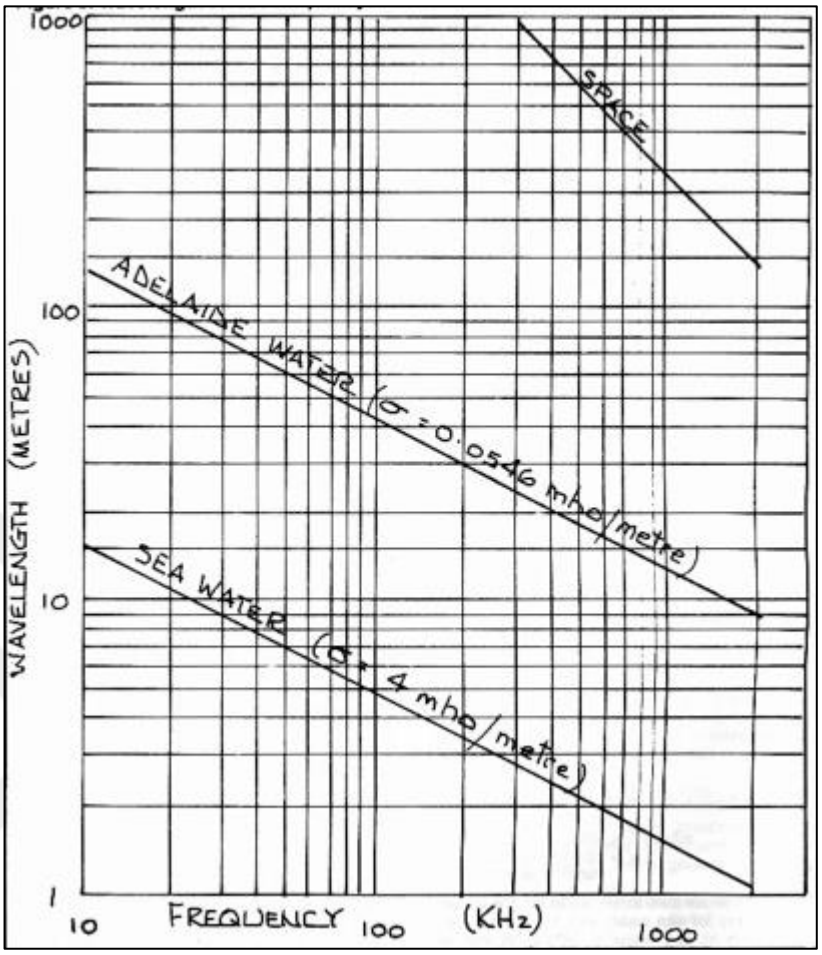

Source: BUTLER, L. 1987. Underwater Radio Communication. Amateur Radio. Melbourne: Wireless Institute of Australia.

As a result, in an aquatic medium, it is very difficult to perform a radio frequency communication (E. J. Hilliard and Gould, 1977). Due to its physical properties, it requires larger antennas and high energy to perform RF communication in the aquatic environment.

2.2.2 ACOUSTIC COMMUNICATION

The term of "underwater wireless communication" is generally used to describe acoustic technologies due to its physical properties in water medium. The water is the ideal sound-propagating medium, because sound wave travels faster in water rather than it travels in the air. Therefore, acoustic communication has been the standard solution for submarine missions. Acoustic communication In 1826, a Swiss physicist Jean Daniel Colladon and

a French mathematician Charles Strum performed an experiment in Lake Geneva, for measuring the speed of sound (Gay-Lussac and Arago, 1827, Medwin and Clay, 1998).

Figure 2.4: Colladon and Strum's apparatus for measuring the speed of sound in the water.

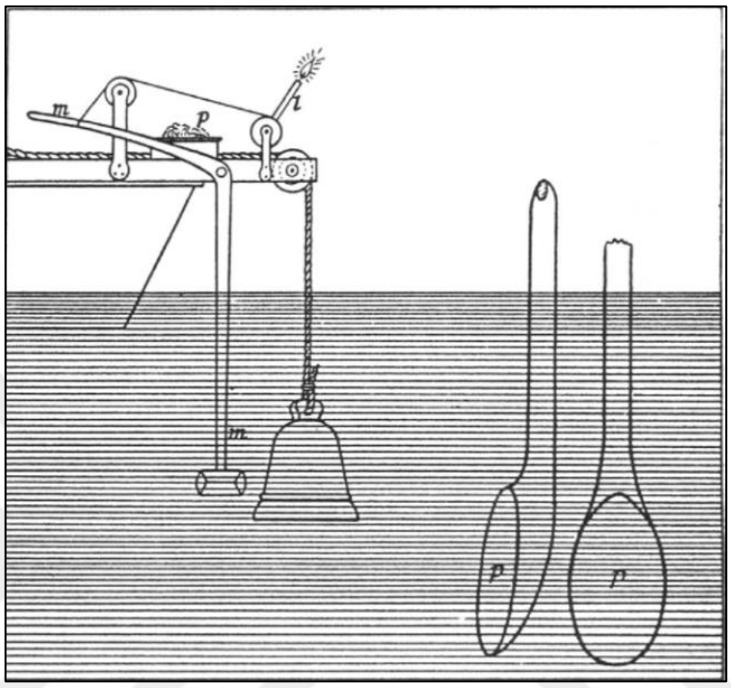

After the experiment, they found the value of 1435 $^{m}/_{s}$, but it was realized that the speed of sound in water varying by other parameters like; salinity, temperature and pressure. In sea water, the speed of the sound is close to 1500 $^{m}/_{s}$, it is also varied by the same parameters (Lurton, 2002). The speed of sound directly related with the physical characteristics of the water it increases with increasing temperature, salinity and pressure (Waite, 2002).

The physical characteristics of water allow to transmit data to long range distances, but it is relative to signal attenuation. The sound wave attenuation occurs due to viscosity and molecular relaxation (Waite, 2002). The attenuation of the sound wave in fresh water and salt water is shown in Figure 2.5. Low salinity means very low attenuation and it also means low propagation losses. The absorption of high frequencies is dominated by the viscosity of the water, on the other, the absorption of low frequencies is dominated by the dissolved compounds in the water (Lanzagorta, 2013). The attenuation due to molecular relaxation is only present in sea water. The molecular absorption is directly related with

dissolved compounds in water, such as boric acid and magnesium carbonate. Temperature, salinity and pressure (directly related to the depth) are the physical characteristics of the medium that affect the attenuation factor in both regimes.

Figure 2.5: Absorption of sound in sea water as a function of frequency $\left(dB/_{Hz}\right)$

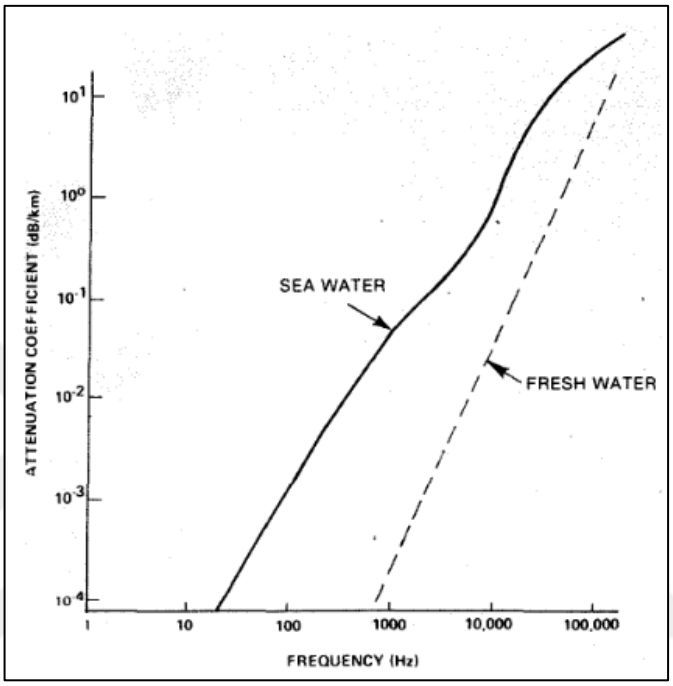

Source: QUAZI, A. & KONRAD, W. 1982. Underwater Acoustic Communications. *IEEE Communications Magazine,* 20**,** 24-30.

Despite the advantage, acoustic communication also carries some problems when the signal transmission speed is important (Liu et al., 2008). However, the sound wave propagation in water medium is highly dependent on frequency (Cochenour et al., 2008). In Table 2.2 the performance of typical acoustic communication systems is summarized.

Table 2.2: Typical Bandwidth Performance of an Acoustic Communication System with Range

Distance	Range (km)	Bandwidth (kHz)	Data Rate
Very Long	>100	<1	~600 bps
Long	10-100	~2-5	~5 kbps
Medium	1-10	~10	~10 kbps
Short	0,1-1	~10-100	~30 kbps
Very Short	<0,1	>100	~500 kbps

Source: COCHENOUR, B. M., MULLEN, L. J. & LAUX, A. E. 2008. Characterization of the Beam-Spread Function for Underwater Wireless Optical Communications Links. IEEE Journal of Oceanic Engineering, 33, 513-521.

Acoustic communications also present other issues, such as sensitivity to multipath propagation, ambient noise and dispersion. Due to long propagation range of acoustic waves, acoustic communication is not a stealthy method to communicate, on the other hand, because of the problems that cited above, it is very difficult to perform a highly directional acoustic communication (Lanzagorta, 2013).

2.2.3 OPTICAL COMMUNICATION

The present technology of RF underwater communication requires huge antenna size, high transmitter power even in fresh water and suffers from high attenuation in the sea. On the other hand, acoustic underwater communication does not require big transceivers and it provides more physical flexibility to its platform. The acoustic signals can reach up to long rage distances due to physical properties of water. Nevertheless, it suffers from high latency and low data rates on long rage communication. It also distresses marine mammals due to utilized communication frequencies. To overcome these problems and to reach high-frequency data rates, optical communication is an obvious choice for underwater communication. However, underwater optical communication is a challenging task, since the optical beams are also suffered from attenuation caused by high absorption and scattering. But for short distances, it is the best solution for voice communication.

Underwater optical communication is still in development, it has some advantages of the RF communication, but not all the disadvantages. The electromagnetic waves vary from each other in lengths and in energy levels. The wavelength (λ), as the name implies, is the distance between two successive wave peaks. The energy levels are inversely proportional to the wavelengths; higher the wavelength, the shorter the energy level. The electromagnetic spectrum, is the arrangement of the electromagnetic waves according to the wavelengths or the energy levels. Light is a part of electromagnetic spectrum. The waves, that can be seen by human eye, are just a small part of electromagnetic spectrum. Figure 2.6 shows the entire electromagnetic spectrum. The wave theory indicates that the speed of light is decreasing in a denser medium, yet the particle theory of Newton says the opposite.

Figure 2.6: The electromagnetic spectrum

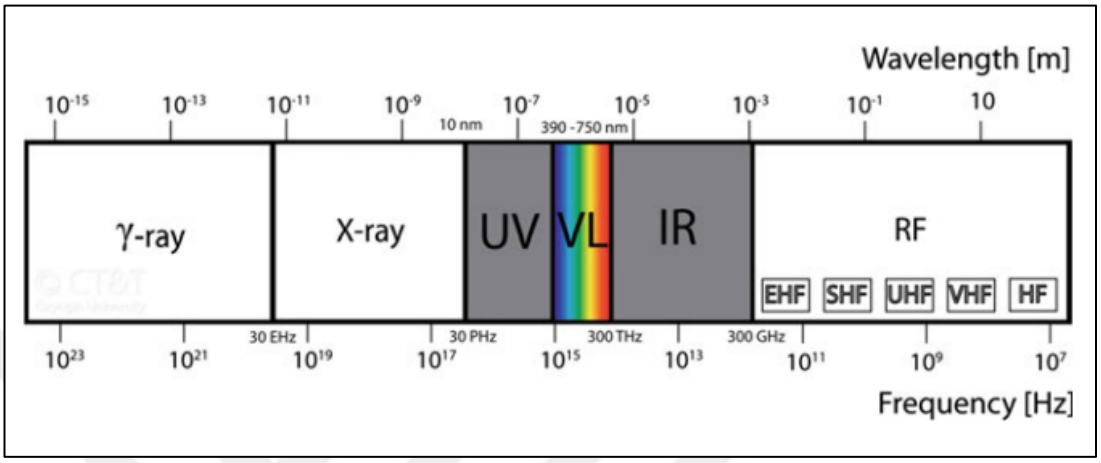

Source: UYSAL, M., CAPSONI, C., GHASSEMLOOY, Z., BOUCOUVALAS, A. C. & UDVARY, E. 2016. Optical wireless communications : an emerging technology. Signals and communication technology,. Switzerland: Springer,.

In the early 1600s, Galileo Galilei attempted to measure the speed of light with his assistant. They tried to measure the speed of light on different hilltops with a known distance between. They use a lantern to generate a light pulse and his assistant opened the shutter of a lantern as soon as he saw the light from Galilei's. They tried the same experiment with different distances between them, unfortunately, they could not manage to measure the speed of light. Galilei concluded that light was too fast to be measured. In 1849, French physicist Armand Fizeau managed to measure the speed of light by his toothed gear setup. He estimated the speed of light $c = 313.300\ {}^{km}/_{s}$. Right after Fizeau, in 1850, French physicist Jean Bernard Léon Foucault replaced the toothed gear with a mirror and he estimated $c = 297.878{,}309\ {}^{km}/_{s}$. Foucault's rotating mirror experiment's purpose was not to physically measure the speed of light in water, yet to perceive what influence a section of water had upon the position of an image light beam. But the more accurate measurement made in 1958 by British Physicist Keith Davy Froome after the invention of radio interferometry and the result was $c = 299.792{,}458\ {}^{km}/_{s}$ in vacuum (Koupelis, 2011).

Figure 2.7: Schematic Outline of Jean Bernard Léon Foucault's the Rotating Mirror Experiment that Determines the Speed of Light in Air and in Water.

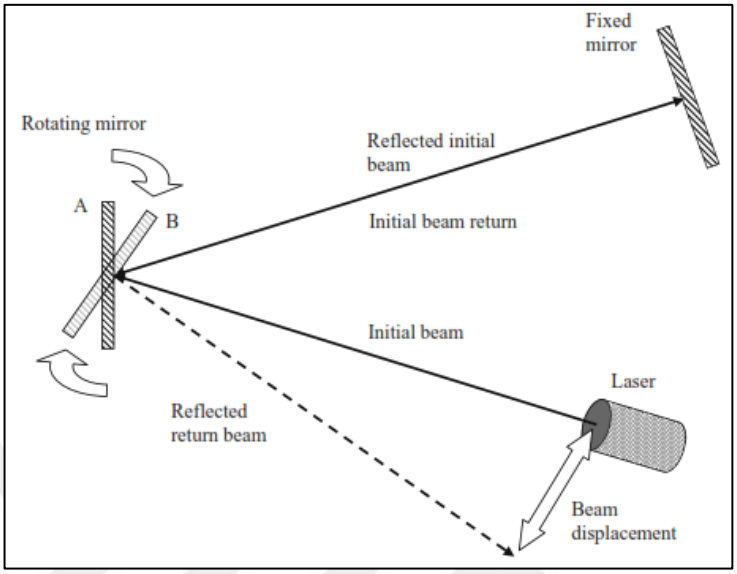

Source: BEECH, M. 2012. The physics of invisibility a story of light and deception. New York, NY: Springer,

In 1621 Dutch mathematician and astronomer Willebrod Snell van Roijen discovered a law for the refraction of light (Beech, 2012). It is known as Snell's Law;

$$n = \frac{c}{V_{medium}} \qquad \textbf{2.6}$$

As it is known the refractive index of water n = 1,33 (Tilton and Taylor, 1938), the speed of light in water; $V_{water} \cong 225.407{,}863\ {}^{km}/_{s}$. Optical communication in water is very tricky due to high attenuation. But water media does not affect light much like other communication methods.

Figure 2.8: Propagation Speeds versus Frequency Calculation in Matlab

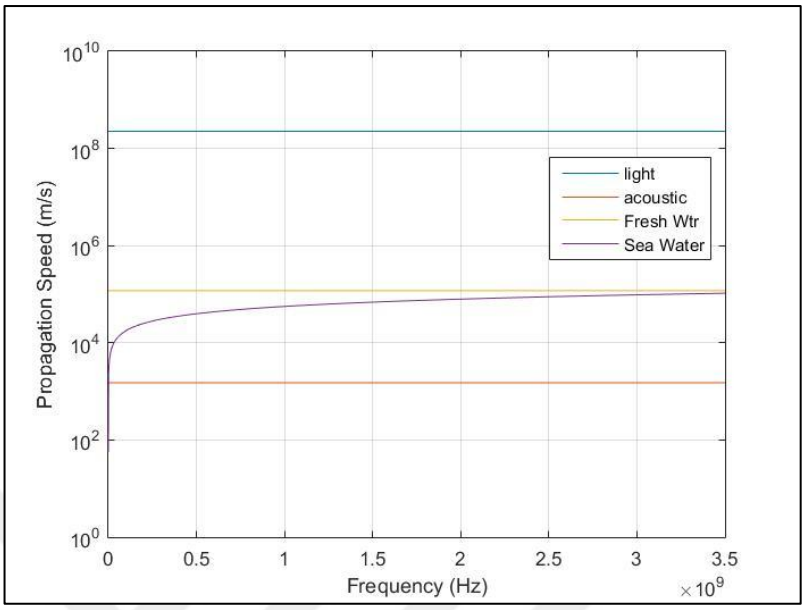

Source: Source Code is given on Appendix A

In Figure 2.8 it is shown propagation speeds versus frequency. Propagating light beam in water medium is subject to intense attenuation due to high absorption and scattering.

The optical properties of the water can be classified as inherent and apparent optical properties (Mobley, 1994). The inherent optical properties characterize optical parameters that only depend on the transmission medium by including the composition of that medium and particle substances present in it (Johnson et al., 2014). This characterization method is independent of light sources. Absorption coefficient, scattering coefficient and attenuation coefficient are the major inherent optical properties of the water (Spinrad et al., 1994). On the other hand, the apparent optical properties depend on not only the transmission medium, but also the geometrical structure of the light sources by including diffusion and collimation (Johnson et al., 2014). Radiance, irradiance and reflectance are the major apparent optical properties of the water (Spinrad et al., 1994). In an underwater communication system, the apparent optical properties are typically used to calculate ambient light levels for communication near the water surfaces, whereas the inherent properties are used to determine the budget of the communication link (Johnson et al., 2014). The inherent properties of the water have a greater impact on the communication link performance. The attenuation coefficient (c) is the most widely

used inherent property. It describes the loss of the optical power per meter and measured in m^{-1}. It is derived by considering the explanations behind the photons that is not reaching to a receiver after being transmitted through an inhomogeneous medium. One reason should be the scattering, and it is considered when the photons is redirected by a refractive index boundary. Alternatively, the photon energy may be converted to heat or be absorbed by chemical contents of the medium and it is known as absorption (Johnson et al., 2014). The overall beam attenuation is consisted from scattering and absorption together. It is determined by Beer-Lambert's Law, where the optical power (I) is based on the transmitted power (I_0) with a distance (d) and the attenuation coefficient (c) (Mobley, 1994).

$$I=I_0 \times e^{-cd} \qquad \textbf{2.7}$$

The exact value of the attenuation coefficient (c) depends on the wavelength (λ) and changes with different types and depth of the water. The form of the absorption and scattering spectra depend on the different biological factors and these are classified by their optical behavior. The absorption of pure water, absorption by chlorophyll-a and absorption by fluvic and humic acids are the main factors of absorption. The chlorophyll-a is the main substance that makes a group of a photosynthesizing microorganism called phytoplankton and the fluvic and humic acids are the main nutrients for phytoplankton (Johnson et al., 2013). The absorption coefficient a(λ);

$$a(\lambda)=a_w(\lambda)+a_h^0 C_h \exp(-k_h\lambda)+a_f^0 C_f \exp(-k_f\lambda)+a_c^0(\lambda)\left({C_c}/{C_c^0}\right)^{0,602} \qquad \textbf{2.8}$$

Where a_w is pure water absorption coefficient in m^{-1}, a_h^0 is the absorption coefficient of humic acid in which equals to $a_h^0 = 18{,}828\ m^2(mg)^{-1}$, C_h is the concentration of humic acid in ${mg}/{m^3}$, k_h is the exponential coefficient of the humic acid in which equals to $k_h = 0{,}01105\ nm^{-1}$, a_f^0 is the absorption coefficient of fluvic acid in which equals to $a_f^0 = 35{,}959\ m^2(mg)^{-1}$, C_f is the concentration of fluvic acid in ${mg}/{m^3}$, k_f is the exponential coefficient of the fluvic acid in which equals to $k_f = 0{,}0189\ nm^{-1}$, a_c^0 is the absorption coefficient of chlorophyll-a in m^{-1} and C_c^0 is the concentration of chlorophyll-a in which equals to $C_c^0 = 1\ {mg}/{m^3}$ (Haltrin, 1999).

Scattering is a change of course of an electromagnetic energy. It weakens the signal by reducing the amounts of photons reaching to the detector. When a photon backscattered photon reaches back to the detector, it travels a much longer path than a photon moving on a straight line, it causes a temporal distortion of the signal. Figure 2.9 shows the forms of scattering in time.

Figure 2.9: Form of Temporal Scattering

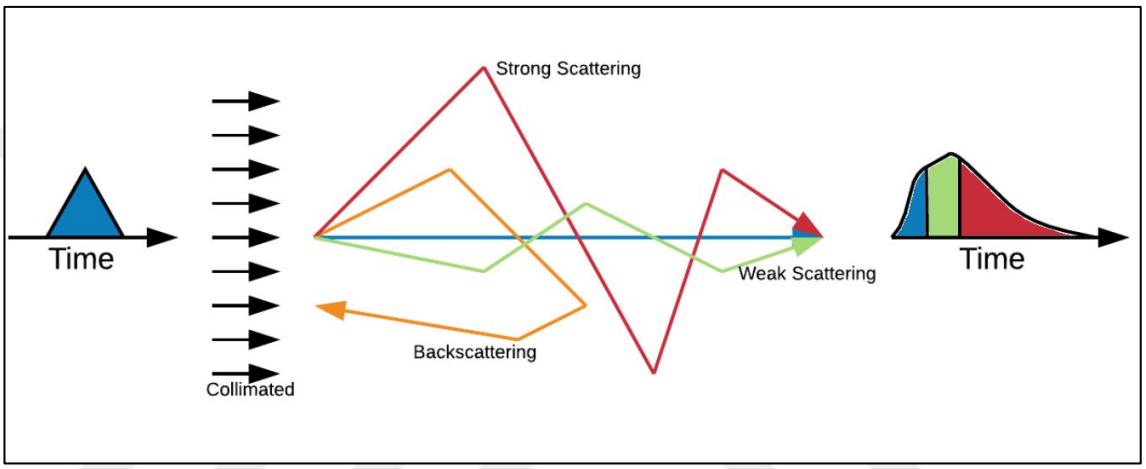

Source: STOTTS, L. B. 1978. Closed form expression for optical pulse broadening in multiple scattering media. Applied Optics, 17, 504-504.

The scattering by the pure water and by particle substance are the two biological factors that influence the scattering spectra. Furthermore, it is separated into small and large particles with a different scattering strength and different statistical distribution (Haltrin, 1999). The scattering b(λ) coefficient equation is given below where the back-scattering coefficient is $b_B(\lambda)$, the pure water scattering coefficient is $b_w(\lambda)$ [m^{-1}], the probability of back-scattering by small particles $b_s(\lambda)$, the probability of back-scattering by large particles is $b_l(\lambda)$, the specific scattering coefficients for small particles $b_s^0(\lambda)$ [$^{m^2}/_{g}$], the specific scattering coefficients for large particles $b_l^0(\lambda)$ [$^{m^2}/_{g}$], the concentration of small particles C_s [$^{g}/_{m^3}$] and the concentration of large particles C_l [$^{g}/_{m^3}$] (Haltrin, 1999).

$$b(\lambda) = b_w(\lambda) + b_s^0(\lambda)C_s + b_l^0(\lambda)C_l \qquad \textbf{2.9}$$

$$b_B(\lambda) = 0{,}5b_w(\lambda) + B_s b_s^0(\lambda)C_s + B_l b_l^0(\lambda)C_l \qquad \textbf{2.10}$$

Where;

$$B_s = 0{,}039\ {}^{m^2}/_{g}\ , B_l = 6{,}4 \times 10^{-4}$$

So;

$$b_w(\lambda) = 0{,}005826\ (m^{-1})\ \left(\frac{400}{\lambda}\right)^{4{,}322}, \quad \textbf{2.11}$$

$$b_s^0(\lambda) = 1{,}151302\ \left(\frac{m^2}{g}\right)\ \left(\frac{400}{\lambda}\right)^{1{,}7}, \quad \textbf{2.12}$$

$$b_l^0(\lambda) = 0{,}341074\ \left(\frac{m^2}{g}\right)\ \left(\frac{400}{\lambda}\right)^{0{,}3}. \quad \textbf{2.13}$$

The effect of scattering on the attenuation coefficient is much less than absorption, except the particulate-rich water types.

In general, there are 4 types of sea water, pure sea water, clear ocean water, coastal ocean water and turbid harbor. In the pure sea waters, absorption is considered as the sum of the absorption in pure water and the absorption in water with a known amount of salt content. The absorption increases with the increase in wavelength. So, the red wavelength is more attenuated than the blue wavelength and for this reason, the deep ocean water is seen rich blue color. In general, ocean waters are rich with dissolved particles like dissolved salts, minerals and organic matters. The first quantitative classification was derived by a Swedish Oceanographer Nils Gunnar JERLOV. The classification splits the ocean as open (clear) ocean water and coastal water. He categorized the clear ocean waters based on their concentration of suspended particles and their geographical locations. It is subdivided into 4 categories, Type IA, IB, II and III. The coastal waters split into groups 1-9, representing the increasing turbidity. These water types have a much higher concentration of dissolved particles where it increases the turbidity level so the effect of absorption and scattering is also increased. The highest concentration of dissolved particles is in the turbid harbors. It limits the propagation of optical beam due to high absorption and high scattering. In Figure 2.10 the distribution of water types over the earth's surface is shown.

Figure 2.10: The global distribution of Jerlov water types.

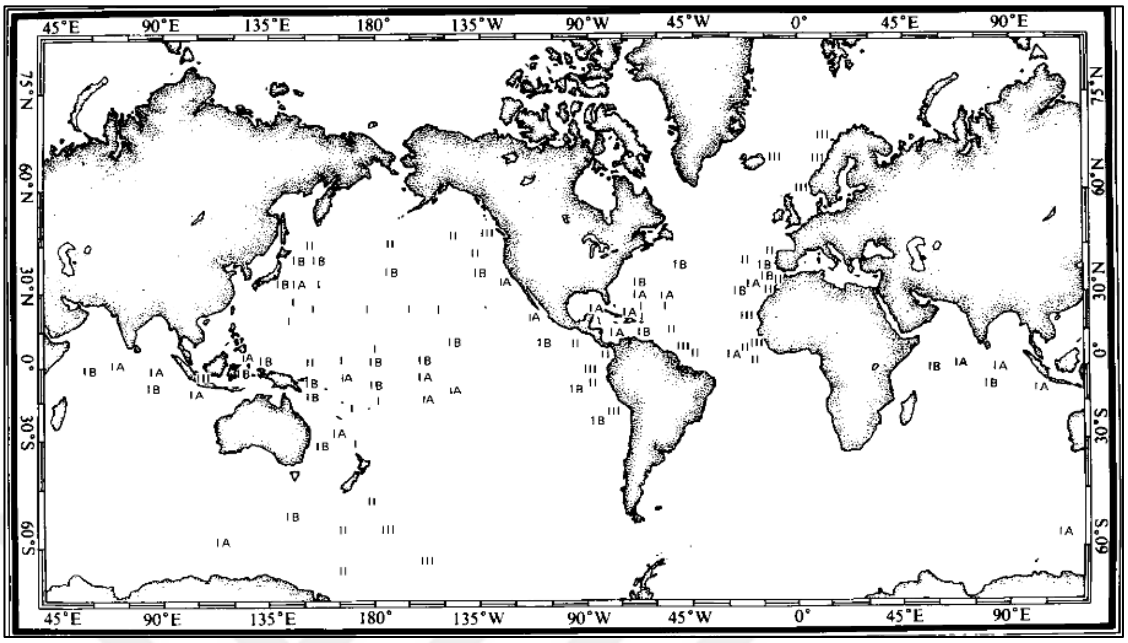

Source: APEL, J. R. 1987. Principles of ocean physics, London ; Orlando, Academic Press.

The term of diffuse attenuation coefficient is the most comprehensive measurements of ocean water quality, due to its ease of measurement. This value simplifies the amount of attenuation for a collimated light beam and so the calculation is made just between the diffuse attenuation coefficient, $K_d(\lambda)$ and the attenuation coefficient, $C(\lambda)$. However, this calculation is not straightforward because, $K_d(\lambda)$ is measured using propagation of solar radiation through the water. The more comprehensive work is done by Jerlov in 1970's. By the help of the knowledge of diffuse attenuation coefficient leads scientists to use many sources of ocean information. In

Figure 2.11 it is shown how various water types (The clear ocean waters are assigned range from cleanest to dirtiest by I-III and the coastal waters are assigned range from 1 to 9.) have a different wavelength dependent diffuse attenuation coefficient.

Figure 2.11: The Diffuse Attenuation Coefficient versus Wavelength Graph for Various Jerlov Water Types.

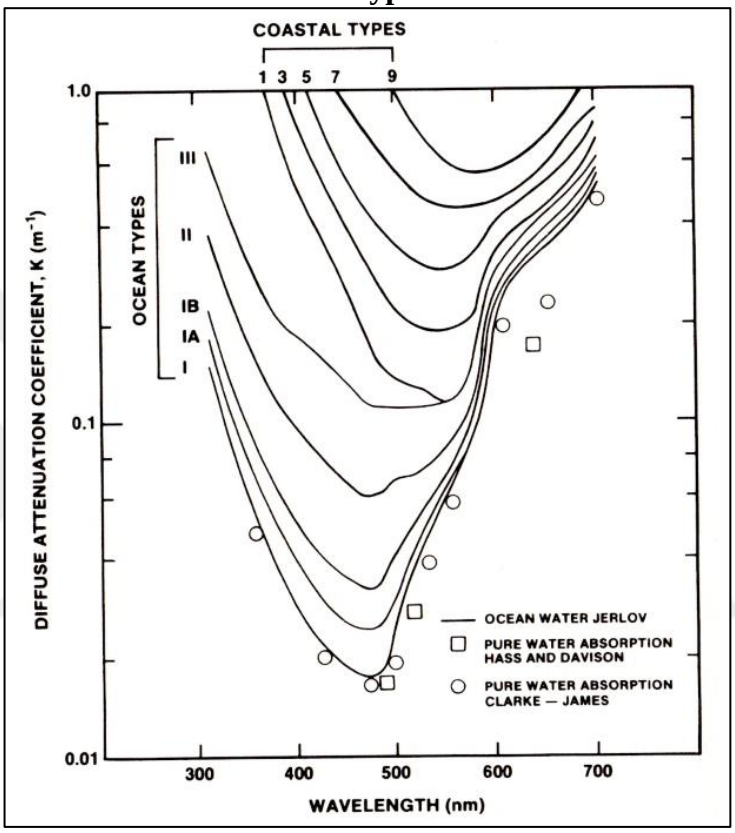

Source: JERLOV, N. G. 1968. Optical oceanography, Amsterdam, New York etc., Elsevier Pub. Co.

The typical values of diffuse attenuation coefficient ($K_d(\lambda)$) associated with wavelength and six major water types are given in Table 2.3.

Table 2.3: Wavelength Dependent Diffuse Attenuation Coefficient for Major Water Types.

λ (nm)	Jerlov Water Types					
	I	IA	IB	II	III	1
350	0,0510	0,0632	0,0782	0,1325	0,2335	0,3345
375	0.0302	0.0412	0.0546	0.1031	0.1935	0.2839
400	0.0217	0.0316	0.0438	0.0878	0.1697	0.2516
425	0.0185	0.0280	0.0395	0.0814	0.1594	0.2374
450	0.0176	0.0257	0.0355	0.0714	0.1381	0.2048
475	0.0184	0.0250	0.0330	0.0620	0.1160	0.1700
500	0.0280	0.0332	0.0396	0.0627	0.1056	0.1486
525	0.0504	0.0545	0.0596	0.0779	0.1120	0.1461
550	0.0640	0.0674	0.0715	0.0863	0.1139	0.1415
575	0.0931	0.0960	0.0995	0.1122	0.1359	0.1596
600	0.2408	0.2437	0.2471	0.2595	0.2826	0.3057
625	0.3174	0.3206	0.3245	0.3389	0.3655	0.3922
650	0.3559	0.3601	0.3652	0.3837	0.4181	0.4525
675	0.4372	0.4410	0.4457	0.4626	0.4942	0.5257
700	0.6513	0.6530	0.6550	0.6623	0.6760	0.6896

Source: JERLOV, N. G. 1976. *Marine optics,* Amsterdam ; New York, Elsevier Scientific Pub. Co.

3. MATERIALS AND METHODS

In this chapter, all the experimental work and setup is explained and all the materials together with all the equipment that are used for the project and for the experiments are listed.

3.1 SYSTEM DESIGN

The prototype consists of one setup that has one transmitter system and one receiver system separately. The system design and its components are shown in Figure 3.1.

Figure 3.1: System Design Schematic

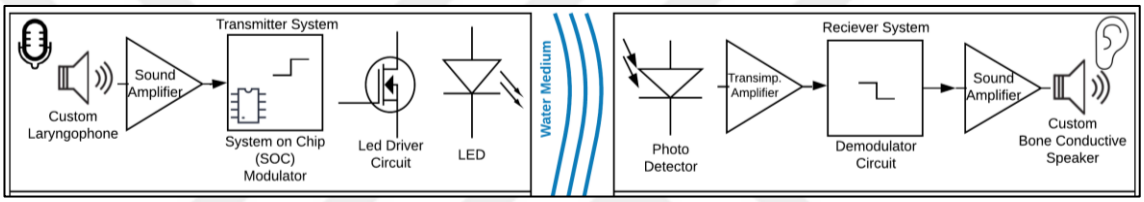

3.2 TRANSMITTER DESIGN

The transmitter system consists of one custom made laryngophone design, one sound amplifier (preamplifier) circuit, one system on chip (SOC) module as the modulator, one led driving circuit and one led.

3.2.1 CUSTOM LARYNGOPHONE

Laryngophone is a type of contact microphone that detects vibrations directly from user's throat, especially from Larynx area that contains the human vocal cords. The Larynx area is shown in Figure 3.2. The advantages of laryngophone are to the sensor capable of picking up speech even in extremely noisy environments, due to its strategical measurement area. Other types of microphones do not function properly under these conditions due to a high level of background noise. As if sound travels much more faster in underwater environmental, laryngophone is the best choice to detect the voice of divers.

Figure 3.2: Human Respiratory Passage Anatomy. (Guyton and Hall, 2006)

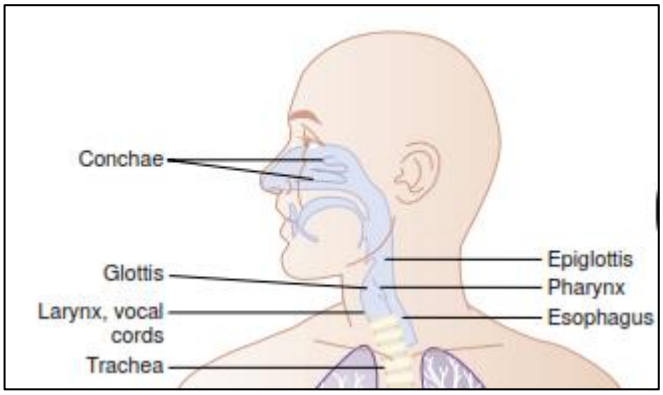

A sufficiently large volume of air and facial mobility are required in order to speak underwater. (Oceanreef, 2010) A full-face mask or a half mask are used by divers to be able to breath underwater environment. By wearing a full-face mask, divers can speak without having any difficulties, on the other hand, speaking with half mask is difficult while the regulator is in the diver's mouth. But full-face masks lead diver to consume much more air compared to when they use a half mask.

In our system, a Kingstate KPEG116 piezo transducer was used to detect voice signals. It has 30 V maximum operating voltage and an operating temperature between -30ºC +85ºC. Since piezo transducers have high impedance, it needs a preamplifier circuit that has a high input impedance.

Figure 3.3: Kingstate KPEG116 Piezo Transducer and Frequency Response Graph

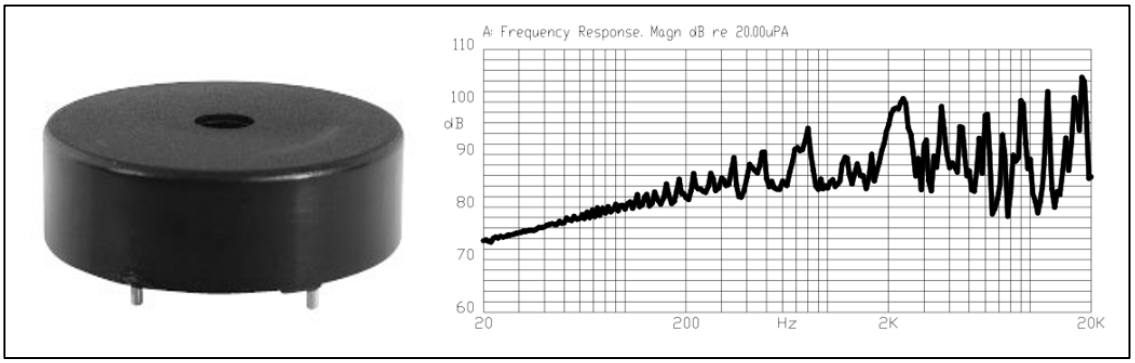

First design made by using BF245A, a JFET transistor that produced for many decades by several companies. But it is now discontinued. BF545A has the same electrical

characteristic with a different electronic package. Both have a very high input impedance and relatively low noise. In ***Figure 3.4*** the schematic of preamplifier circuit is shown.

Figure 3.4: Schematic of Preamplifier Circuit

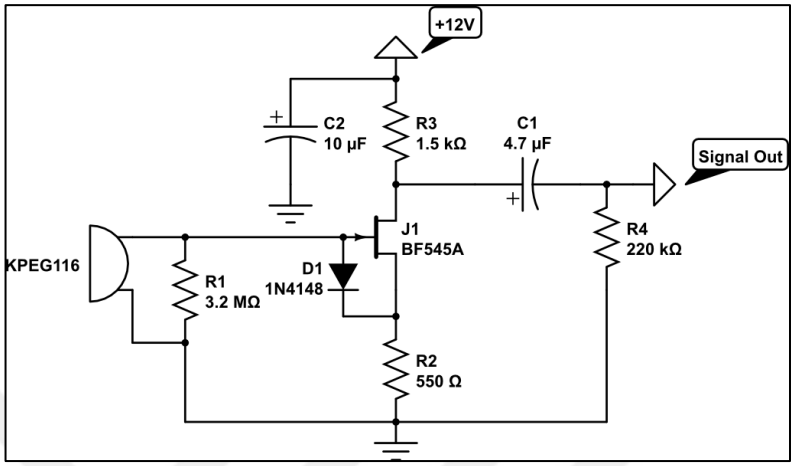

The finished design is shown in Figure 3.5.

Figure 3.5: Custom Design Laryngophone

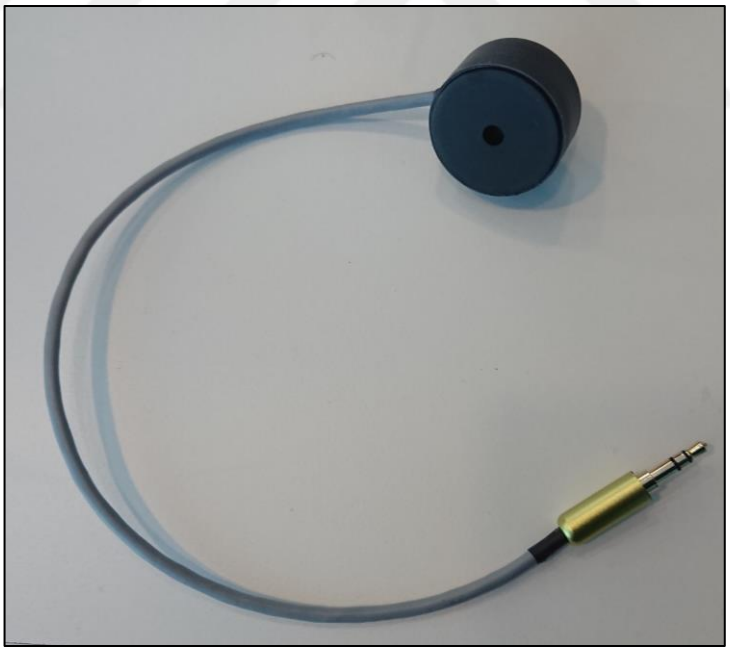

3.2.2 Transmitter Circuit

Transmitter circuit consists of three parts. One microcontroller for quantizing analog signal, one led driver circuit and one led to transmit signal. Most of the microcontrollers have an Analog to Digital Converter to quantize an analog signal. Microcontrollers are

capable of detecting Transistor to Transistor Logic (TTL) binary signals. In electronics binary 1 signal represents the supply voltage of the microcontroller and binary 0 signal represents ground of the microcontroller. Binary signals are digital signals that can only be detected by a digital input of the microcontroller. An analog to digital converter (ADC) is a useful feature that converts an analog voltage signal to a digital number.

Arduino Pro Mini is a microcontroller board that designed with Atmega328. It has 14 digital input/output pins, 6 analog inputs, an on-board oscillator and an onboard regulator. Arduino is an open-source platform based on easy to use software and hardware. In Figure 3.6 Arduino Pro Mini development board and its pinout are shown. In Appendix B the open source circuit schematic of Arduino Pro Mini development board is given.

Figure 3.6: Arduino Pro Mini Development Board with Pin Outs

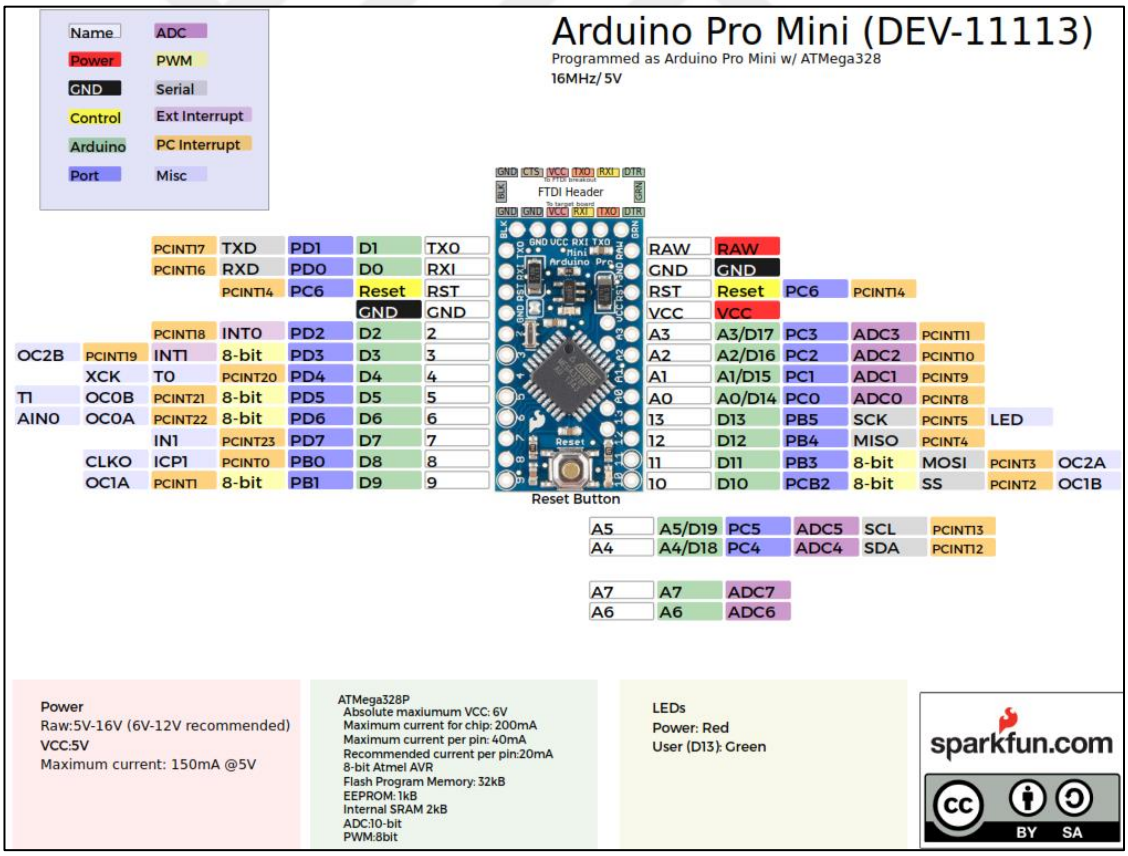

Source: SPARKFUN. 2014. Graphical Datasheet of Arduino Pro Mini 328 - 5V/16MHz [Online]. Sparkfun. Available: https://cdn.sparkfun.com/datasheets/Dev/Arduino/Boards/ProMini16MHzv1.pdf [Accessed 2017].

Table 3.1: Technical Specifications of Arduino Pro Mini Development Board

Microcontroller	ATmega328
Power Range	5-12 V
Operation Voltage	5V
Digital I/O Pins	14 (6 are PWM capable)
UART	1
SPI	1
I2C	1
Analog Input Pins	6
Max. DC current per I/O pin	40 mA
Flash Memory	32 KB
SRAM	2 KB
EEPROM	1 KB
Clock Speed	16 MHz

Not every pin of a microcontroller has an ability to do analog digital conversions. On Arduino Pro Mini board, ADC pins have an "A" in front of its label (A0 to A5). Atmega328 microcontroller has a 10-bit analog to digital conversion capability. It means, it can measure 1024 (2^{10}) discrete analog levels. The ADC has a fairly complex working principle. The most common technique uses the analog voltage to charge an internal capacitor, once the capacitor is charged, it starts to discharge across an internal resistor and the capacitor discharge time measured. The microcontroller monitors the number of clock cycles that have passed before the capacitor is discharged and when the ADC is complete, this number of cycles is returned. The ADC value is a ratio metric value; ADC assumes 5V is 1023 and anything lower than 5V is the ratio between 5V and 1023.

$$\frac{resolution\ of\ the\ ADC\ (1023)}{System\ Voltage\ (5V)} = \frac{ADC\ Reading\ (x)}{Analog\ Voltage\ Measured\ (y)} \qquad \textbf{3.1}$$

For sampling a high impedance, signal Data Input Disable Register (DIDR) of the microcontroller is used. The DIDR is an ADC register that disconnects the digital inputs from the necessary ADC channels. An analog signal causes an electromagnetic interference and it leads the digital input to constantly toggle high and low. It creates excessive noise near the ADC channel. The digital inputs and ADC have an internal capacitance, and what if DIDR not used in ADC process, it will slow down the frequency of the input signal. In general, Arduino does not use DIDR, but it can be activated by adding "DIDR0 = 0x01;" in code. It activates DIDR on analog 0 channel. Atmega328 can work with ADC clock frequency up to 500kHz. By the help of the datasheet of

Atmega328, for setting the sampling frequency “ADCSRA = 0xe5;” which needs to be added to the code. It sets the ADC to clock frequency/32, where the clock frequency is 16MHz resulting in 500kHz sampling frequency.

Once the analog signal is quantized, it is needed to be create a driving Pulse Width Modulation (PWM) signal to drive the LED. Atmega328 has a versatile of PWM usage. Simply PWM is a voltage control method, at fixed cycles the amount of power corresponding to the power that system needs for the output. In ***Figure 3.7*** the PWM signal shown with constant remaining cycles.

Figure 3.7: PWM Signal

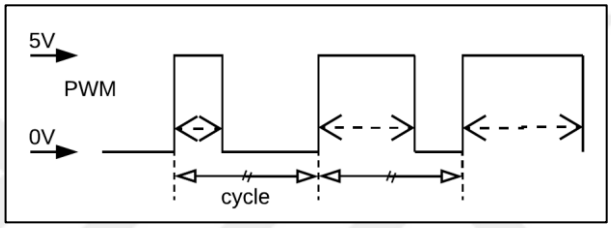

In the system PWM signal is used to generate a carrier frequency to the voice signal. Normally Voltage Controlled Oscillators (VCO) are used for frequency modulation (FM) or phase modulation (PM). But VCO circuits are more complicated rather than microcontrollers. It requires discrete components to setup the carrier frequency. In ***Figure 3.8*** the FM modulation on a PWM modulation is shown. The signal is now inside a Phase Locked Loop (PLL) with a constant cycle. PLLs are commonly used to generate, modulate, demodulate, filter or recover a noisy signal.

Figure 3.8: PWM with Frequency Modulation

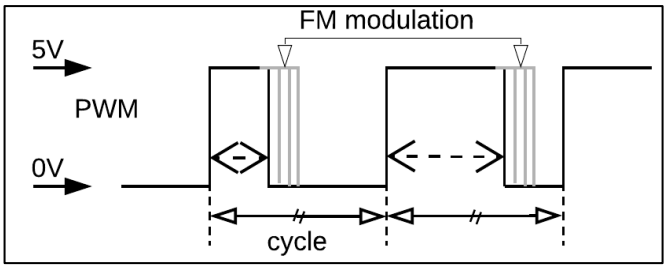

In this system, a Pulse Frequency like Modulation (PFM) is used. It is more energy efficient and most likely the inverse of PWM signals. In Figure 3.9 the difference between PWM and PFM like signals are shown with Frequency Modulation. Arduino is not

capable of generating high frequency PFM like signals. By using an inverting MOSFET, the circuit now is capable of converting PWM signal into PFM like signal.

Figure 3.9: PWM versus PFM like Signal and with Frequency Modulation

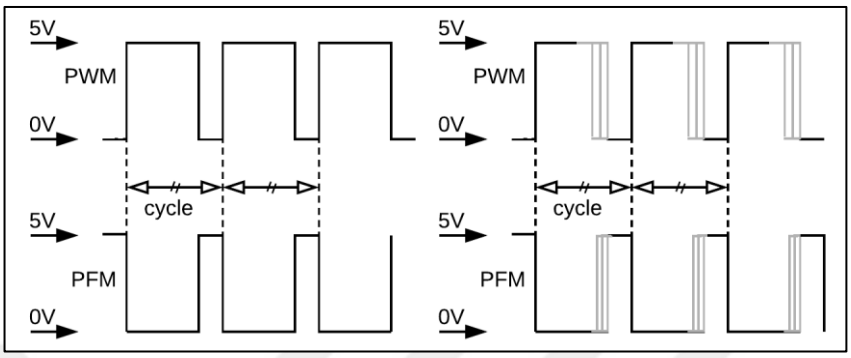

The cycle length is the same for each signal value, and this is set as the MAX value that the counter will handle. It is also called the resolution of the signal and determined as the duty cycle. The MAX value is 255 and the lower value is 0 for Atmega328, therefore, with 8-bit resolution, 256 possible positions can be obtained by 2^8. The higher MAX value means the higher bit depth, but it lowers the frequency. Arduino is capable of generating 12 different PWM frequencies with 12 different bit depths. In ***Table 3.2*** it is shown the different PWM frequencies with corresponding bit depths and "PWM_FREQ" that is needed to be assigned in code.

Figure 3.10: Carrier Frequency, Original Signal and Modulated Signal Chart

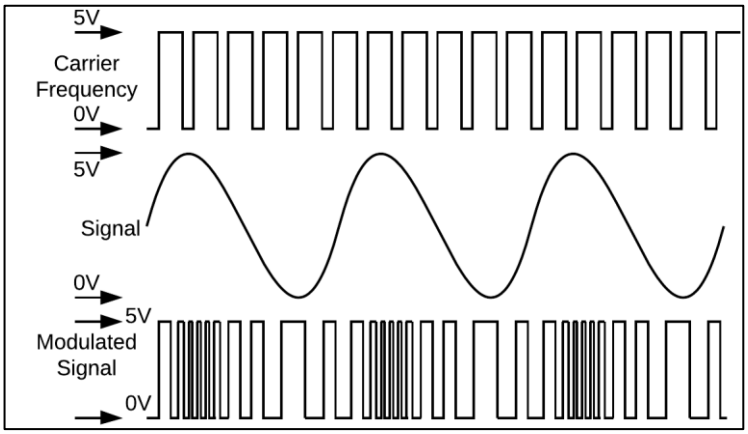

Table 3.2: The PWM Frequencies with Corresponding Bit Depths and Code Settings

	Fast – PWM_MODE 1		
Frequency	**PWM_FREQ**	**Bit Depth**	
Fcpu=16 MHz	**Value**	**Single**	**Dual**
250 kHz	0x003F	6-bit	12-bit
125 kHz	0x007F	7-bit	14-bit
62,5 kHz	**0x00FF**	**8-bit**	**16-bit**
31,3 kHz	0x01FF	9-bit	N/A
15,6 kHz	0x03FF	10-bit	N/A
7,81 kHz	0x07FF	11-bit	N/A
3,91 kHz	0x0FFF	12-bit	N/A
1,95 kHz	0x1FFF	13-bit	N/A
976 Hz	0x3FFF	14-bit	N/A
488 Hz	0x7FFF	15-bit	N/A
244 Hz	0xFFFF	16-bit	N/A
122 Hz	N/A	N/A	N/A

The 62,5 kHz is the most suitable frequency that can be chosen. It is above the human hearing frequency of 20 kHz and it has the 8-bit and 16-bit depth options when a single or dual PWM used. Dual PWMs are the mixture of an upper and lower value to generate one analog signal. It most likely corrects the signal errors and leads high resolution signal. The code is written in C language and Arduino sketch is used to compile and upload the code to microcontroller board. The written C code is given in Appendix C section. The electronic schematic of transmitter circuit is shown in Figure 3.11.

Figure 3.11: The Schematic of Transmitter Circuit.

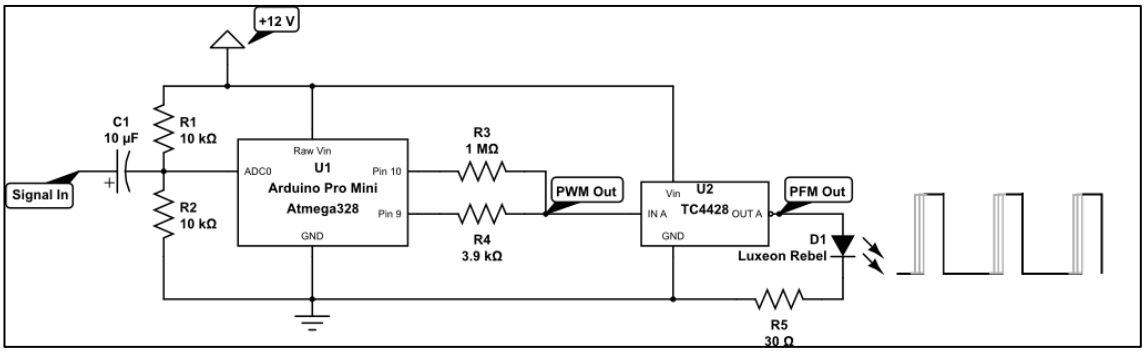

3.2.3 LED

The wavelength of the LED is very important for underwater optical communication. The wavelength is directly correlated with the diffuse attenuation coefficient. For

determination of λ, the April 2013 data set of Aqua MODIS satellite are used. The coordinates of data are 39° 4'48.00"N and 26°39'36.00"S, between Lesbos Island and Turkey in the Aegean Sea. (***Figure 3.12***)

The attenuation coefficient is calculated with empirical formulas. To derivate K_d, in 1981, Austion and Petzold made a linearization to a sample data of irradiance and radiance. (Austion and Petzold, 1981)

$$\overrightarrow{K_d}(\lambda) = K_w(\lambda) + A\left[\frac{L_w(\lambda_1)}{L_w(\lambda_2)}\right]^B \qquad \textbf{3.2}$$

Where, $= 0{,}15645$, $L_w = {R_{rs}(\lambda)}/{E_d(\lambda)}$, $B = -1{,}5401$, λ=488 nm is the wavelength that K_d will be calculated, λ_1 = 555 nm and λ_2 = 488 nm are two wavelengths within the blue-green spectral region, $K_w(488\sim490) = 0{,}016\ m^{-1}$ is the pure water diffuse attenuation coefficient in 488 nm.

$$\overrightarrow{K_d}(488) = 0{,}016 + 0{,}15645 \times \left[\frac{R_{rs}(488)E_d(488)}{R_{rs}(555)E_d(555)}\right]^{-1{,}5401}$$

(3.3)

Note that ${E_d(488)}/{E_d(555)}$ is approximately equal to 1,03, because the value for different sun angles at the surface varies slightly. (Lee et al., 2005) $R_{rs}(488) = 0{,}00463\ sr^{-1}$ and $R_{rs}(555) = 0{,}00166\ sr^{-1}$ are taken from the data of Aqua Modis Satellite. (***Figure 3.13***)

$$\overrightarrow{K_d}(488) = 0{,}016 + 0{,}15645 \times \left[1{,}03 \times \frac{0{,}00463}{0{,}00166}\right]^{-1{,}5401} = 0{,}04679\ m^{-1} \qquad \textbf{3.4}$$

Figure 3.12: The Location and The Data Set of April 2013 Aqua Modis Satellite.

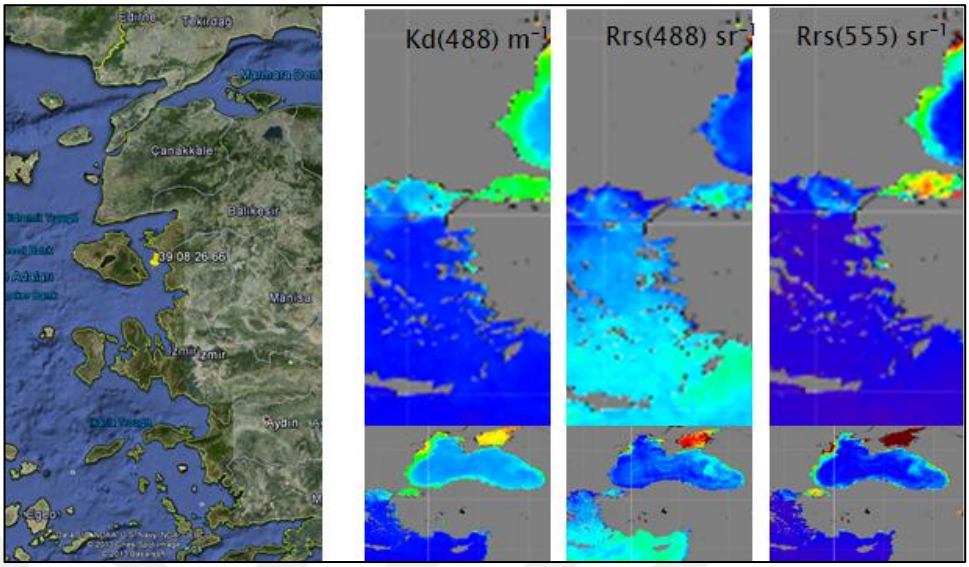

Figure 3.13: The Display of Data Set of April 2013 Aqua Modis Satellite.

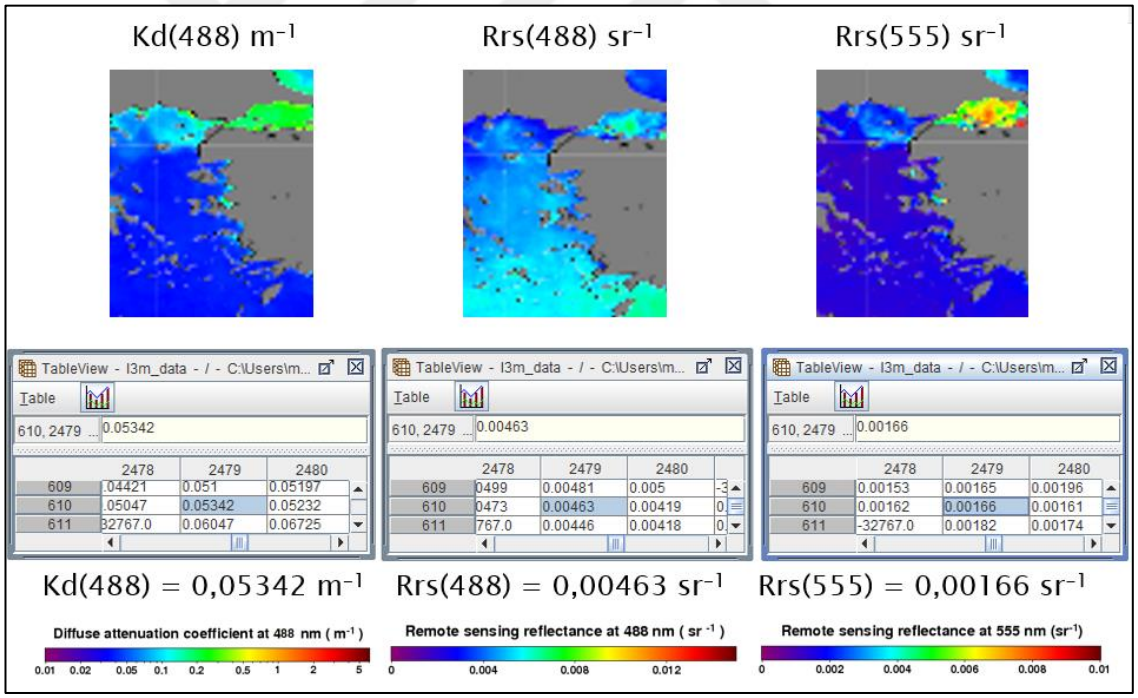

It is seen that calculated $\overrightarrow{K_d}(488)$ value is 0,04679 m^{-1} and the satellite data value of $\overrightarrow{K_d}(488)$ is 0,05342 m^{-1}. The approximation is around ±0,00663. For these coordinates, it is determined from Table 2.3 that Aegean Sea is water type IB for 500nm wavelength.

The spectra of downwelling irradiance In Figure 3.14 the irradiance/transmittance versus wavelength graphic is given for each water types. When it is compared with wavelength

dependent diffuse attenuation coefficient of Jerlov, (Table 2.3) 505 nm is the optimal wavelength that can be chosen for the application.

Figure 3.14: Graphic of Irradiance/Transmittance versus Wavelength on Different Water Types.

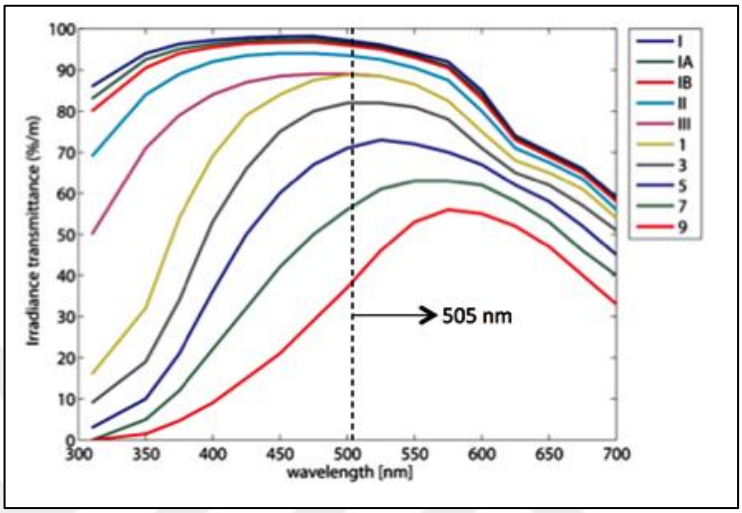

Source: JERLOV, N. G. 1976. *Marine optics,* Amsterdam ; New York, Elsevier Scientific Pub. Co.

For each prototype one LCML-PE01-0070 Luxeon Rebel High Power Cyan Led is used.

Figure 3.15: Luxeon Rebel LED (LXML-PE01-0070)

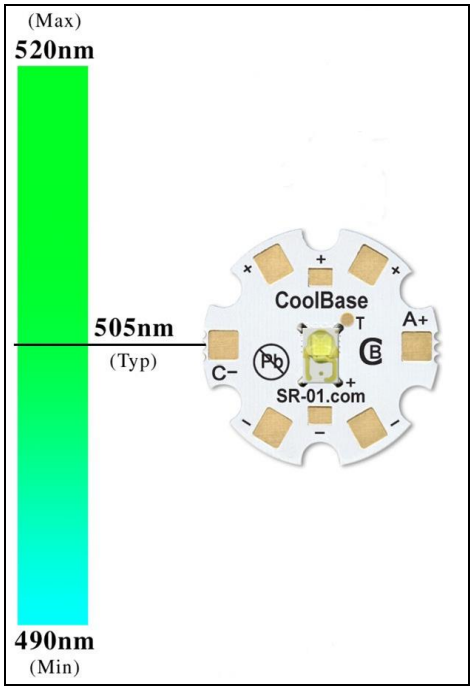

Table 3.3: LXML-PE01-0070 Luxeon LED Specifications

LED Color	Cyan
Lumens @ 350 mA	76
Lumens @ 700 mA	122
Efficacy (lm/W) @ 350mA	75
Efficacy (lm/W) @ 700mA	51
Typical Wavelength (nm)	490 to 520
Wavelength Range (nm)	505
Beam Angle	125
Recommended Operating Current (mA)	700
Maximum Rated Drive Current (mA)	1000
Typical Forward Voltage (Vf)	3.25
Maximum Forward Voltage (Vf)	3.51
Thermal Resistance (C°/W)	10
Maximum Junction Temperature (C°)	150
Operating Temperature Range (C°)	-40-135
Dimensions L x W x H (mm)	4.5 x 3 x 2

The laws of Lambert and Beer also can be used for calculating the weakening of the light under the water.(Bazeille et al., 2012) The Beer-Lambert law is given by:

$$I_{\lambda,d} = I_{\lambda,0} \times e^{-K_\lambda d} \qquad \textbf{3.5}$$

Where, λ is the wavelength, $I_{\lambda,d}$ is the intensity of light with λ wavelength at a distance d from the light source, $I_{\lambda,0}$ is the intensity of light with λ wavelength at the light source. Since the intensity and the beam angle of the LED are respectively 76 lumens and 125º, it gives 656,3 lux for 1 centimeter distance.

Figure 3.16: The Light Intensity versus Distances of LED plotted from Matlab Code

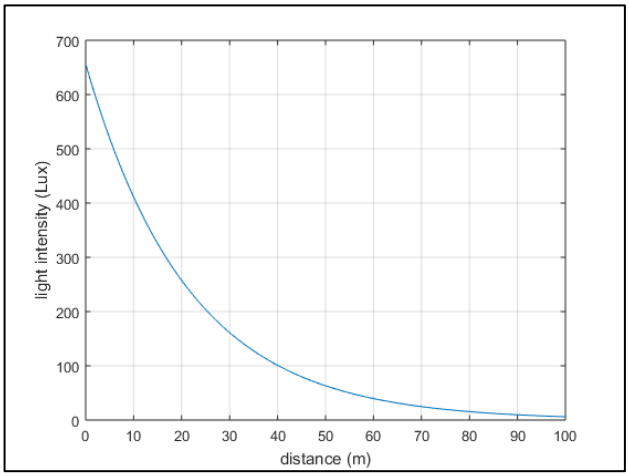

Source: Source Code is given Appendix D

For getting better results, it is needed to decrease the beam angle, so a OPC1-2-COL reflector is used on the LEDs. It reduces the LED output beam angle to 13^{o}.

Figure 3.17: OPC1-2-COL Reflector Photo and Size Chart.

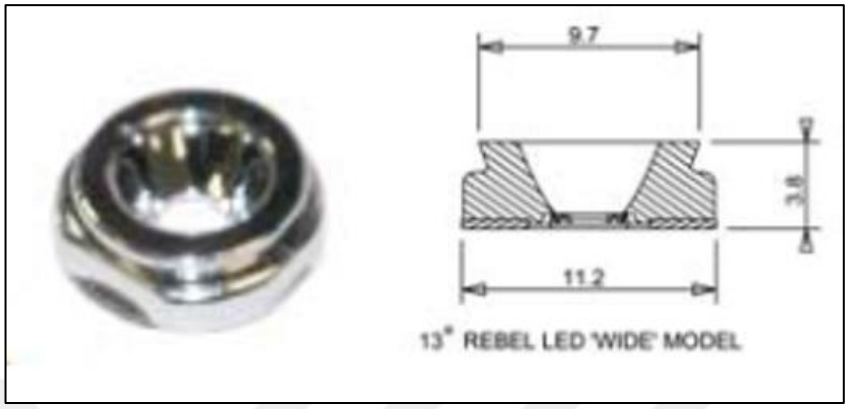

Figure 3.18: Finished Transmitter Unit

3.3 Receiver Design

The receiver system consists of one custom made photo detector array, one transimpedance amplifier (preamplifier) circuit, one signal conditioning and demodulator circuit, one sound amplifier circuit and a custom-made bone conductive speaker design.

3.3.1 Custom Photo Detector Array

Photodiodes are very small photo-voltaic cells. Typically, they have a much smaller surface area to minimize the capacitance and they are optimized to minimize leakage

currents and noise. When a photon hits the surface of a photodiode, electrons start to mobilize by producing currents which is proportional to the number of photons.

Photodiodes are available in a variety of sizes from the “small area” to the “large area”. The difference between these is the surface area size of the silicon substrate that effects the device capacitance. The small area photodiodes are mostly used in high-speed receivers due to its low capacitance. The low capacitance allows better frequency response. Most of the silicon photodiodes have the best optical response in the near-infrared wavelengths around 750-900 nm, but they still have a reasonable optical response in the lower portion of the spectrum.

The silicon-based PIN photodiode BPW34 is very common in the market. It has a variety of usage due to wide range spectral response, low internal capacitance, low price and market availability. The spectral response of BPW34 is given on **Figure 3.20**.

Figure 3.19: Silicon Based PIN Photodiode BPW34

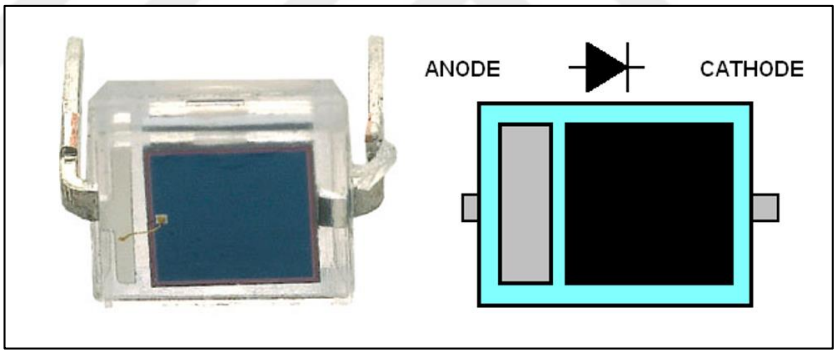

Figure 3.20: The Spectral Response of BPW34

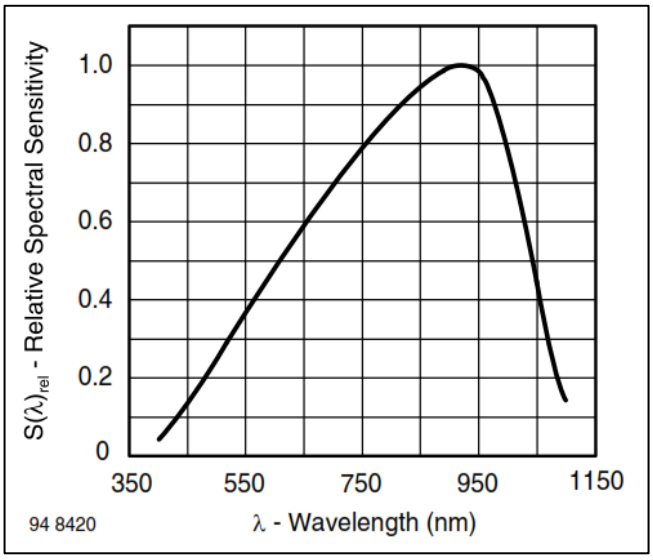

The radiant sensitive area of BPW34 is 7.5 mm^2. Four BPW34 are connected in parallel for increasing the surface area to 30 mm^2. It also increases the internal capacitance to 160 pF, that it is directly related to receiver frequency capability. One can note that the capacitance value did not cause any problem with receiving frequency. The electrical characteristics of BPW34 are listed in Table 3.4.

Table 3.4: The Electrical Characteristics of BPW34

Parameters	Test Conditions	Min.	Typ.	Max.
Breakdown Voltage	I_R=100 uA	60 V	-	-
Reverse Dark Current	V_R=10 V	-	2 nA	30 nA
Diode Capacitance	V_R=3 V, f=1 MHz	-	25 pF	40 pF
Range of Spectral Bandwidth	-	-	430 to 1100 nm	-
Rise Time	V_R=10 V, R_L=1 kohm, λ= 820 nm	-	100 ns	-
Fall Time	V_R=10 V, R_L=1 kohm, λ= 820 nm		100 ns	

Figure 3.21: Photodiode Array Design

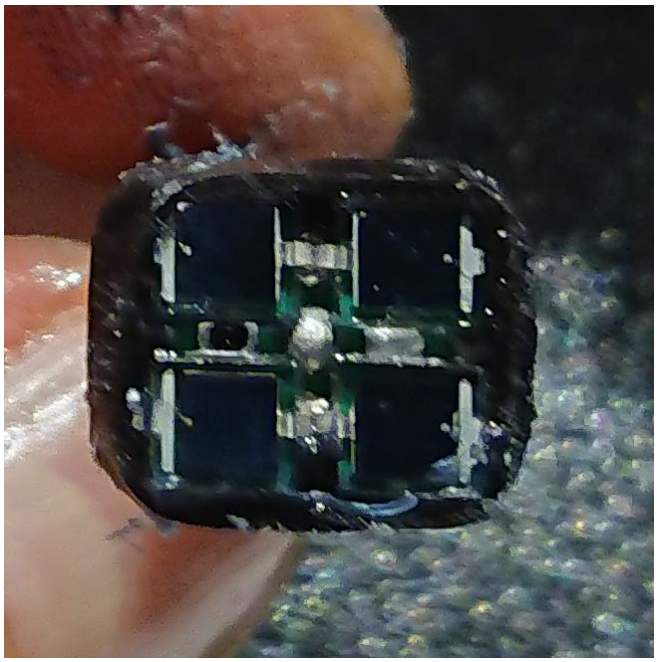

3.3.2 Receiver Circuit

The receiver circuit consists of three parts. A photodetector with preamplifier, signal conditioning, demodulation and sound amplifier. The receiver circuit design is shown in Figure 3.22.

Figure 3.22: Receiver Circuit

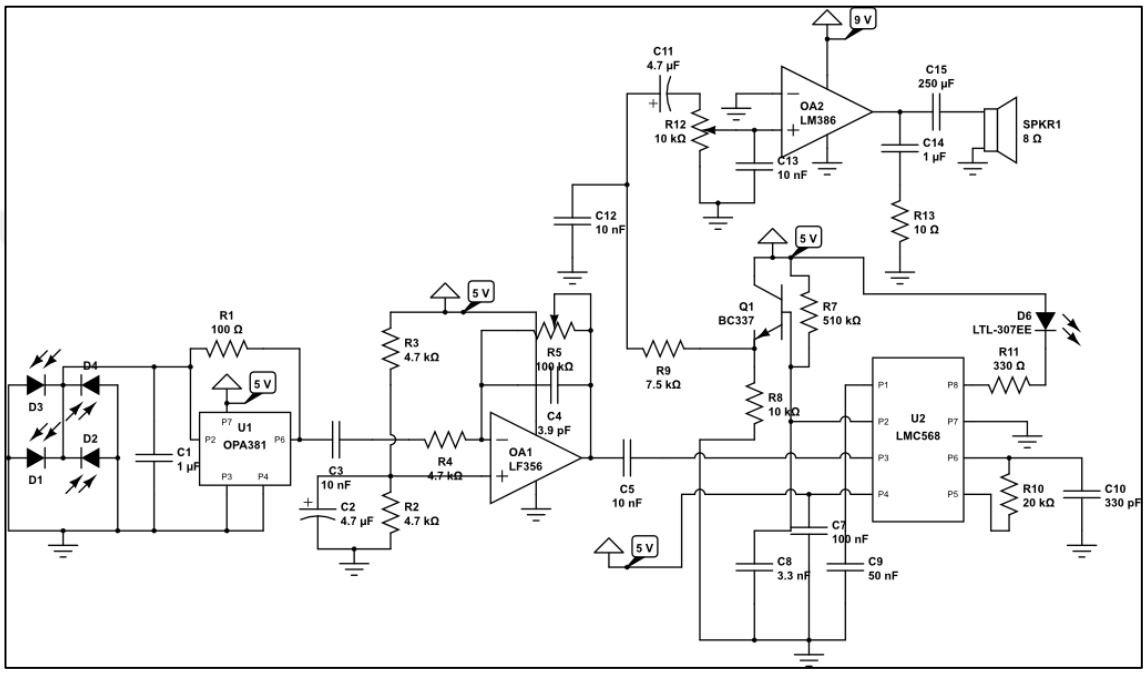

To acquire a good quality signal with a photodiode, it is needed to use an amplifier to boost the signal. A transimpedance amplifier is the most suitable amplifier method that can be used. When a current is provided to the input of the transimpedance amplifier, it produces a voltage proportional to its input current. OPA381 has over 250kHz transimpedance bandwidth with high precision and with very low 1/f noise. Photodiodes will source around 200µA, OPA381 offers a low impedance input and it allows to apply enough conversation gain to boost the signal and converts it to voltage. The basic circuit example is given on Figure 3.23.

Figure 3.23: OPA381 Datasheet Transimpedance Amplifier

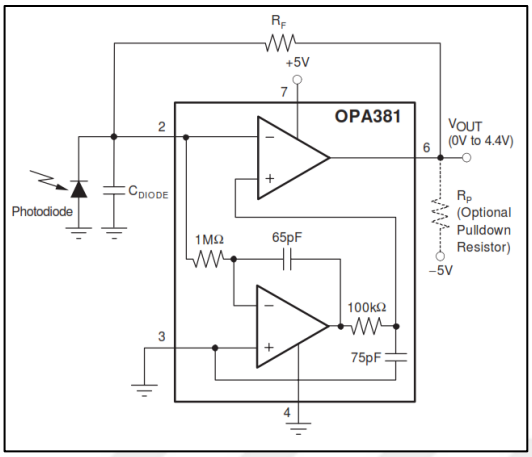

After the signal acquired from the transimpedance amplifier, a high precision JFET input operational amplifier LF356 is used for conditioning the signal. When the modulated signal acquired, it enters to LMC568. LMC568 is a low power phase locked loop integrated circuit. A phase locked loop (PLL) is a circuit makes a specific framework that track with another. A PLL consists of a phase detector and a voltage controlled oscillator. The input signal is compared with the phase of the voltage controlled oscillator output, by the phase detector and an error signal is produced. In all applications, the PLL circuit tracks the phase of the input signal, locks it and demodulates the signal. The reference circuit design is taken from the datasheet of LMC568. After the demodulated signal is obtained, pure voice communication signal, it is needed to be amplified.

Figure 3.24: LMC568 Low Power Phase Locked Loop Datasheet Example Circuit

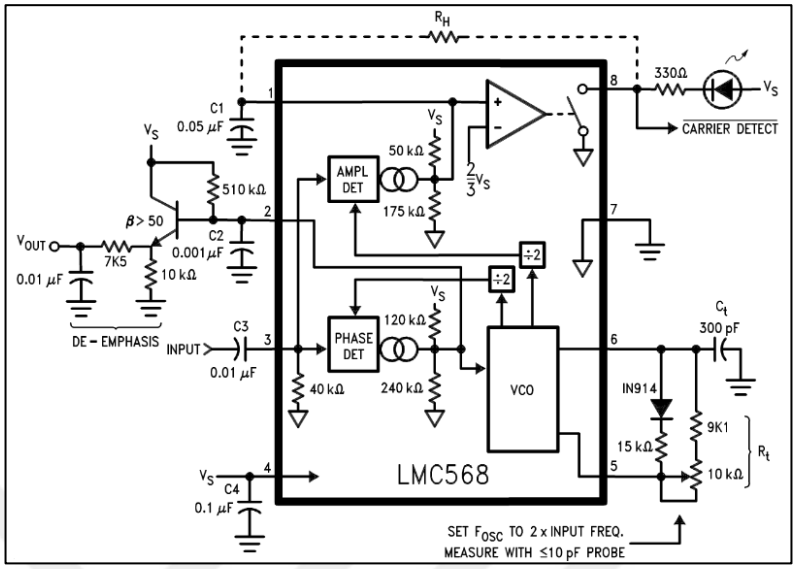

LM386 is a low voltage audio power amplifier that is used to amplify demodulated signal. The LM386 is a mono channel audio amplifier that can drive speakers from 4 to 32 ohms. On Figure 3.25 typical application of LM386 is given with the reference circuit design that is taken from the datasheet of LM386. The reference circuit has an internal gain of 20 dB that is enough to drive 4 ohms bone conductive speaker.

Figure 3.25: LM386 Datasheet Example Circuit

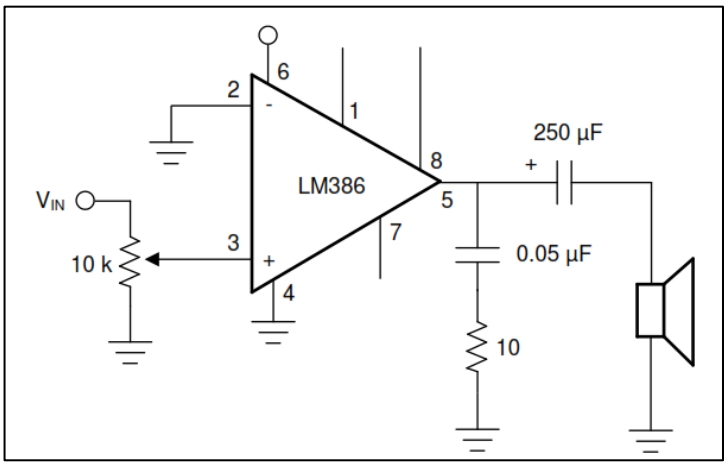

Unlike conventional speakers that produce vibrations to move the air generating a sound signal, bone conductive speakers convert the electrical signal into mechanical vibrations to move a solid surface to generate a sound signal. The solid surface in our case is the

skull of the diver. Vibrations are interpreted by the diver's brain as the sound. The impedance – phase relation of the speaker is given in Figure 3.27.

Figure 3.26: Dayton BCE-1 Bone Conductive Speaker

Figure 3.27: Impedance / Phase graph of Dayton BCE-1 Bone Conductive Speaker

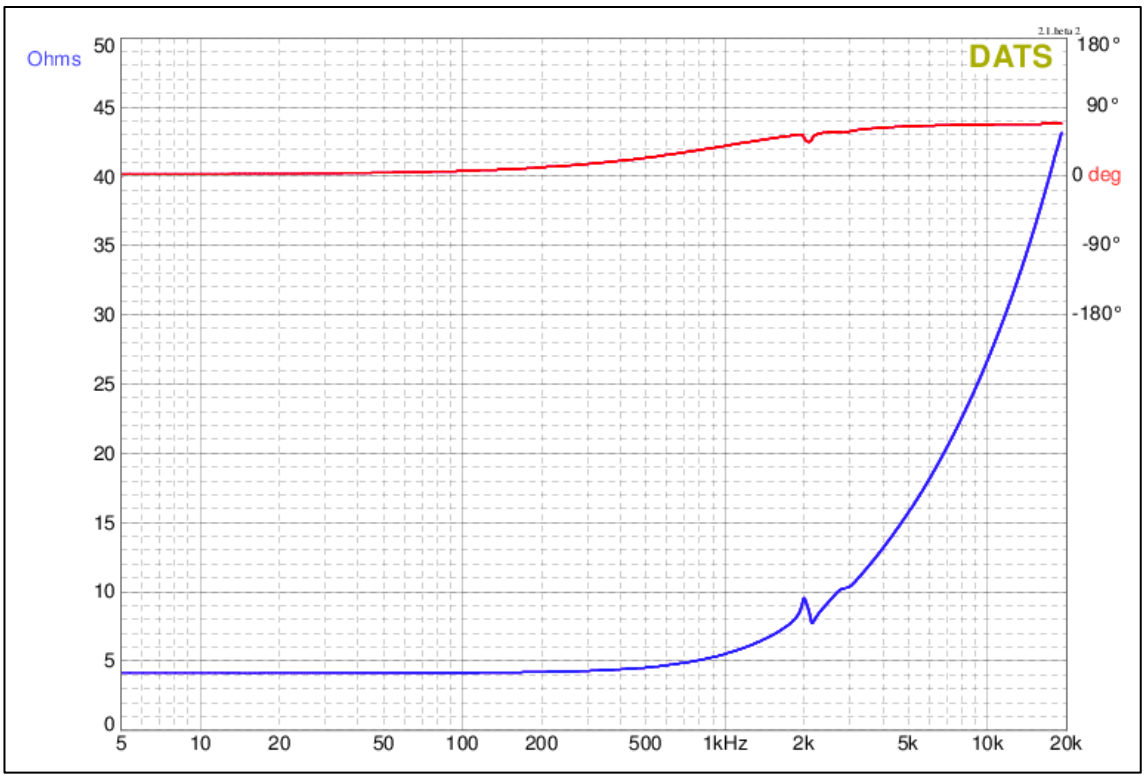

4. OBSERVATIONS

Test results are obtained in laboratory conditions. In first part, electrical signal test and optical wavelength transmission tests are made. In second part, one transmitter and one receiver units are placed 15 meters distance facing each other. The test is made verbally by two operators. One was speaking on the transmitter side and the other one was listening from the receiver side's bone conductive speaker.

4.1 Test Equipment

The following test equipments are used;

- Bitscope Micro Oscilloscope and Analyzer,
- Ocean Optics USB4000 Spectrophotometer,

Bitscope Micro Oscilloscope and Analyzer is used to test electrical signals of the circuit; like modulator frequency, demodulator frequency, transmitter signal, receiver signal and sound signal. The test measurements are shown in Section 4.4 and 4.5.

Figure 4.1: Bitscope Micro Oscilloscope and Analyzer

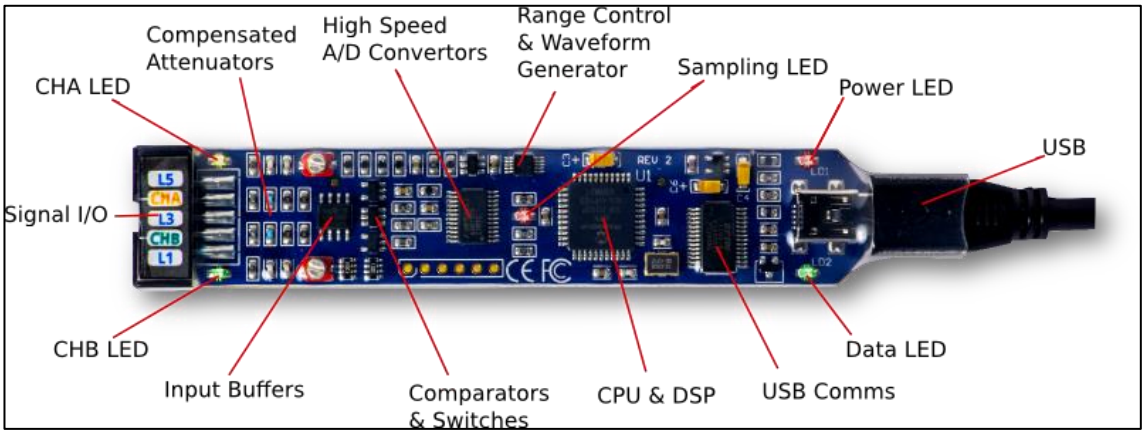

BitScope Micro is a compact sized USB powered mixed signal oscilloscope with following specifications;

- 2 analog inputs,
- 20MHz measurement bandwidth,
- 2 analog comparator channels,

- 6 logic analyzer input with 40 MSps Logic capture,
- Decodes Serial, I2C and SPI interfaces,
- Open Source Software.

Ocean Optics USB4000 Spectrophotometer is used to test the wavelength of the LED and filter's optical wavelength permeability. On the test; light sources are placed 2 cm distance from the optical input of the USB4000 Spectrophotometer and filters are placed between the optical input and the light sources.

Figure 4.2: Ocean Optics USB4000 Spectrophotometer

The USB4000 is a product of Ocean Optics company. It is a spectrometer with following specifications;

- 200-1100 nm detection range,
- 8 x 200 µm pixel size,
- 3648 pixels,
- ~0,1-10 nm optical resolution,
- 16 bits A/D resolution,

4.2 LED Test

As it is mentioned on Section 3.2.3, LED wavelength is important for underwater communication. On this section, Luxeon Rebel LED (LXML-PE01-0070) is tested for the center wavelength of 505nm. As it is seen on Figure 4.3 graph, the peak wavelength is on 505 nm.

Figure 4.3: LED Spectral Graph

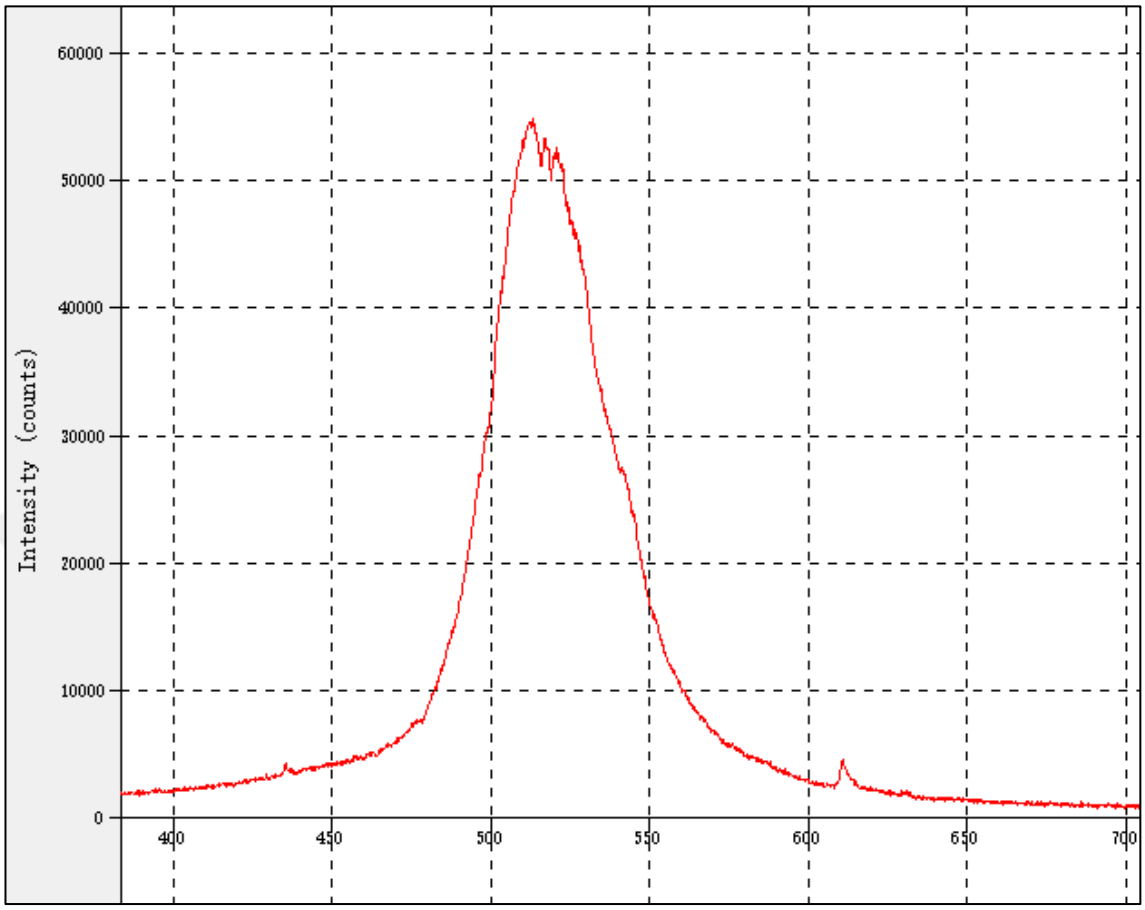

LED test completed after the required values obtained correctly.

4.3 Filter Test

BPW34 has a wide range spectral response. For preventing the noise will be occurred because of other wavelengths, it is needed to design an optical filter. Optical bandpass filters mostly are expensive. On filter test, blue and green transparent acetate films are tested for wavelength permeability. For the test Phillips 9006 HB4 Light Bulb is used to simulate sun light.

Figure 4.4: Phillips 9006 HB4 Light Bulb is used to Simulate Sun Light

The spectral response graph of the Phillips 9006 light bulb is shown on

Figure 4.5 and the spectral response graph of the direct sunlight is shown on

Figure ***4.6***. These measurements are made by Ocean Optics USB4000. The relative spectral response graph of the sunlight is shown on Figure 4.7, and the measurement is made by Ralph Stair in 1954 by a 935 phototube. (Stair, 1954).

Figure 4.5: Spectral Response Graph of Phillips 9006 Light Bulb

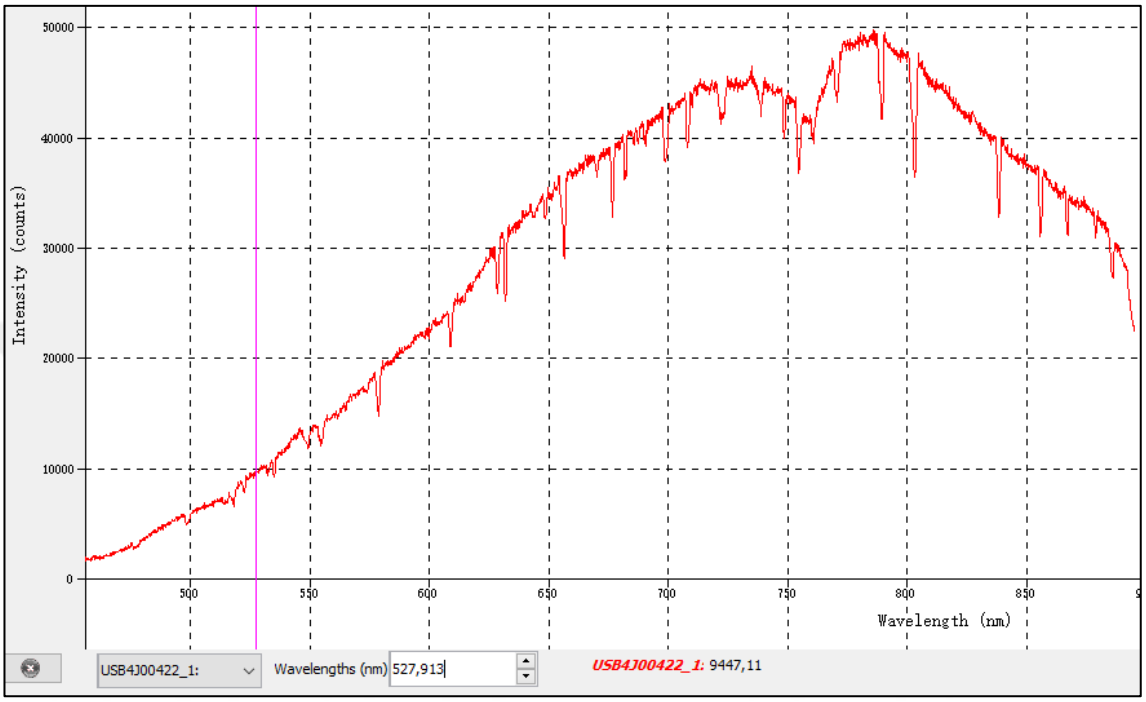

Figure 4.6: Spectral Response Graph of Direct Sun Light

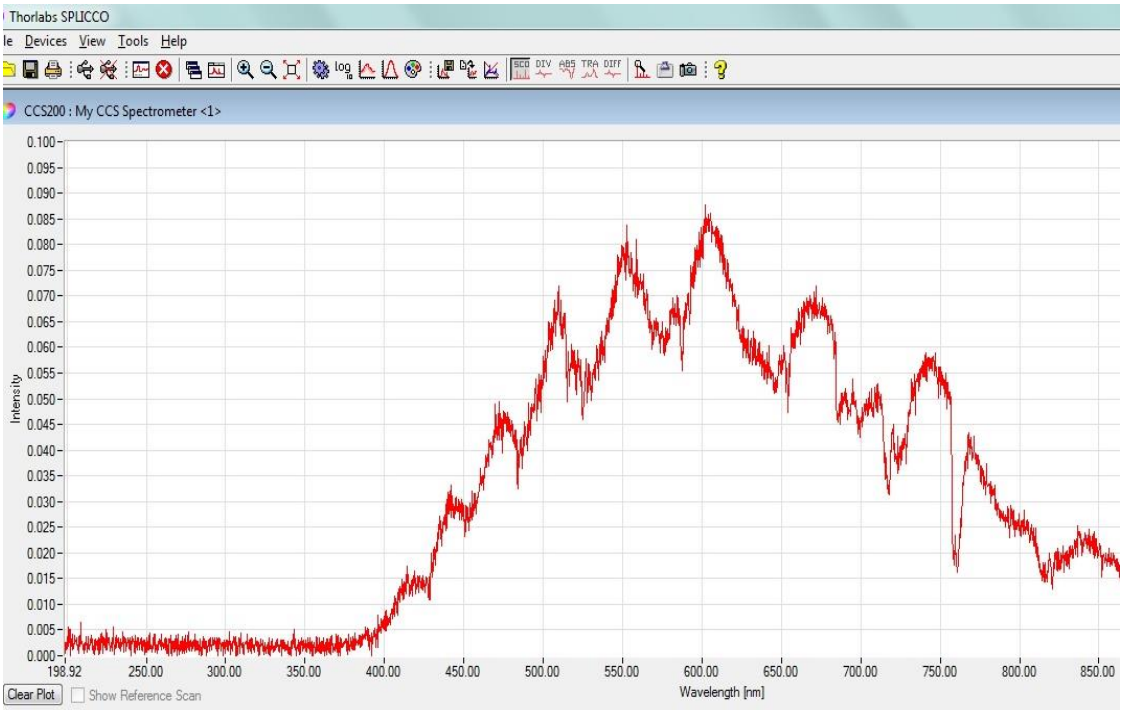

Figure 4.7: Relative Spectral Response Graph of Direct Sun Light Cited on Literature

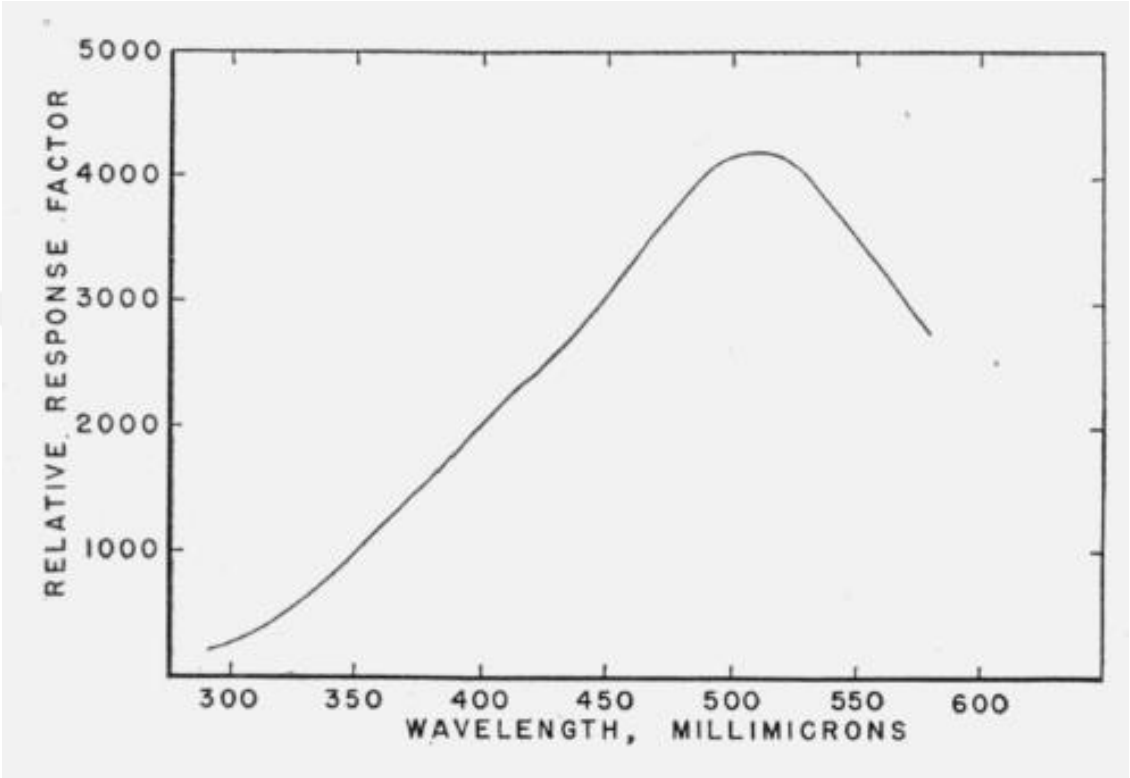

As all the spectral responses were similar, Phillips 9006 HB4 was an ideal light source to simulate the sun light.

The center wavelength of the transmitter LED is 505nm, which is between blue and green wavelength bands. The blue acetate film is tested and its optical attenuation is obtained between 550 nm and 750 nm.

Figure 4.8: Blue Acetate Film Filter

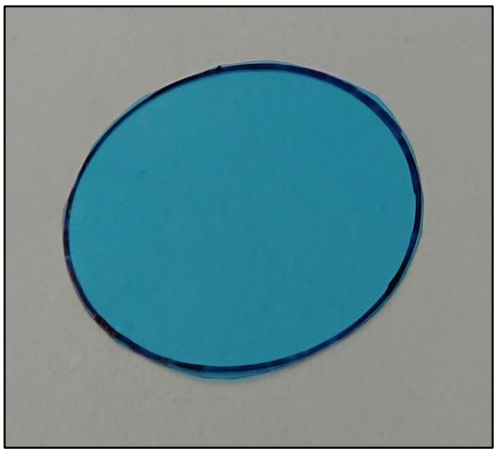

Figure 4.9: Blue Acetate Film's Spectral Graph

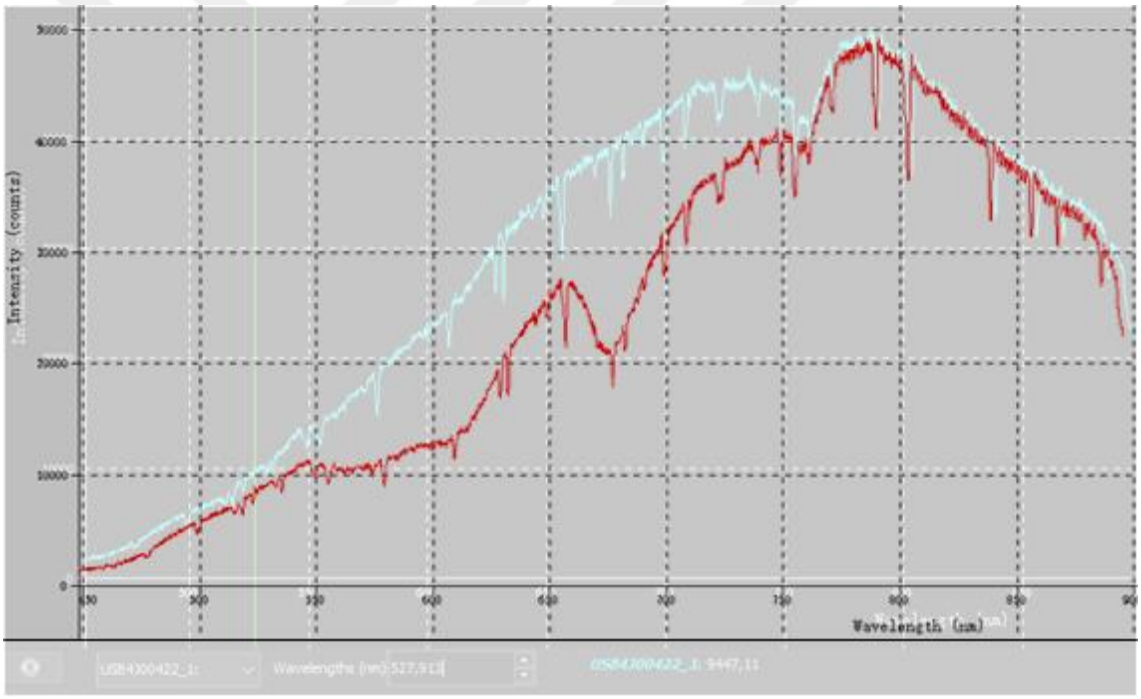

On the

Figure ***4.9***, the cyan colored signal is the spectral response graph of the light bulb Phillips 9006 and the red colored signal is the actual blue acetate measurement.

Green acetate film is tested and its optical attenuation is obtained between 550-900 nm wavelength band and it is most efficient when it is compared with blue acetate film.

Figure 4.10: Green Acetate Film Filter

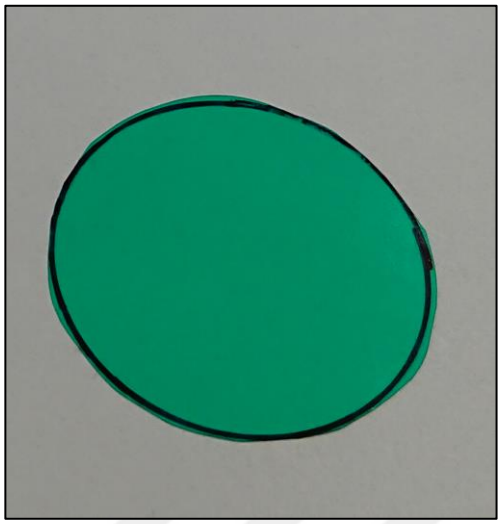

Figure 4.11: Green Acetate Film's Spectral Graph

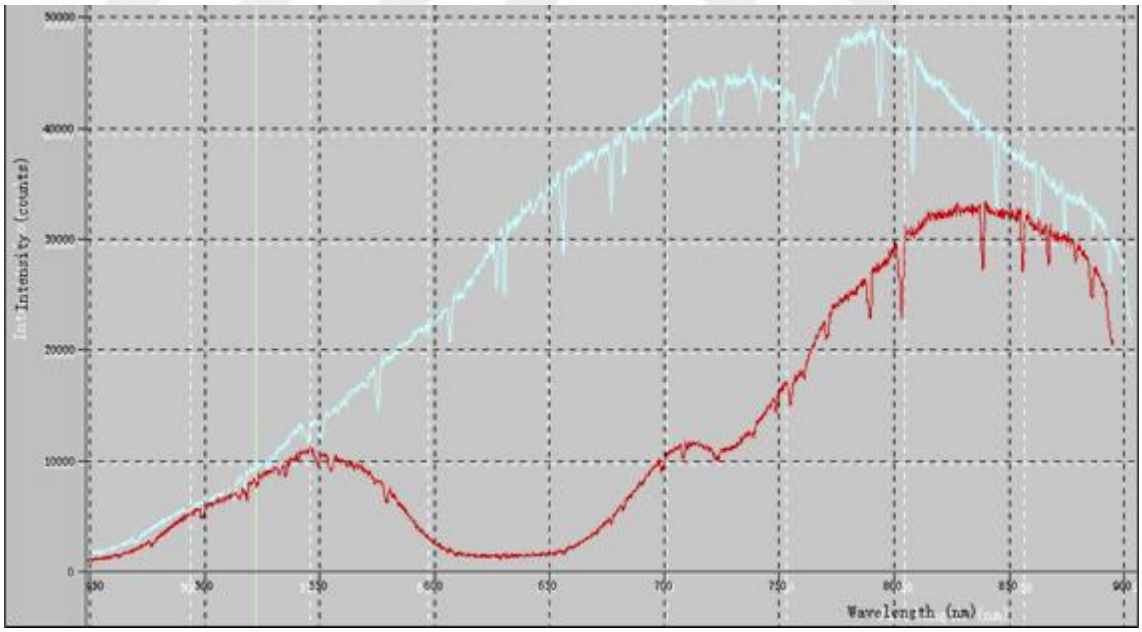

On the Figure 4.11, the cyan colored signal is the spectral response graph of the light bulb Phillips 9006 and the red colored signal is the actual green acetate measurement.

Blue and green acetate films are tested and optical attenuation is obtained between 550-900 nm wavelength band. The result was mostly like green acetate film result, but the effect of blue acetate was also observed at 650-700 nm wavelength band.

Figure 4.12: Blue and Green Acetate Films

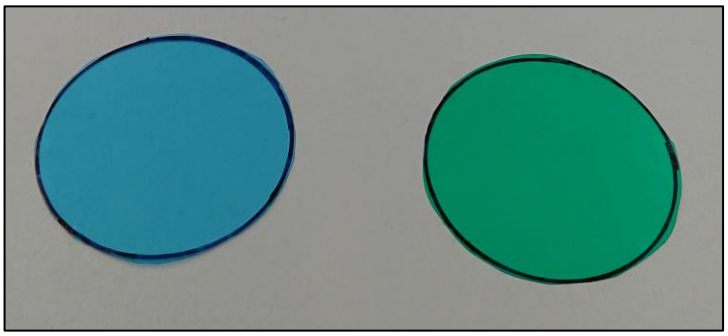

Figure 4.13: Spectral Graph of Blue and Green Acetate

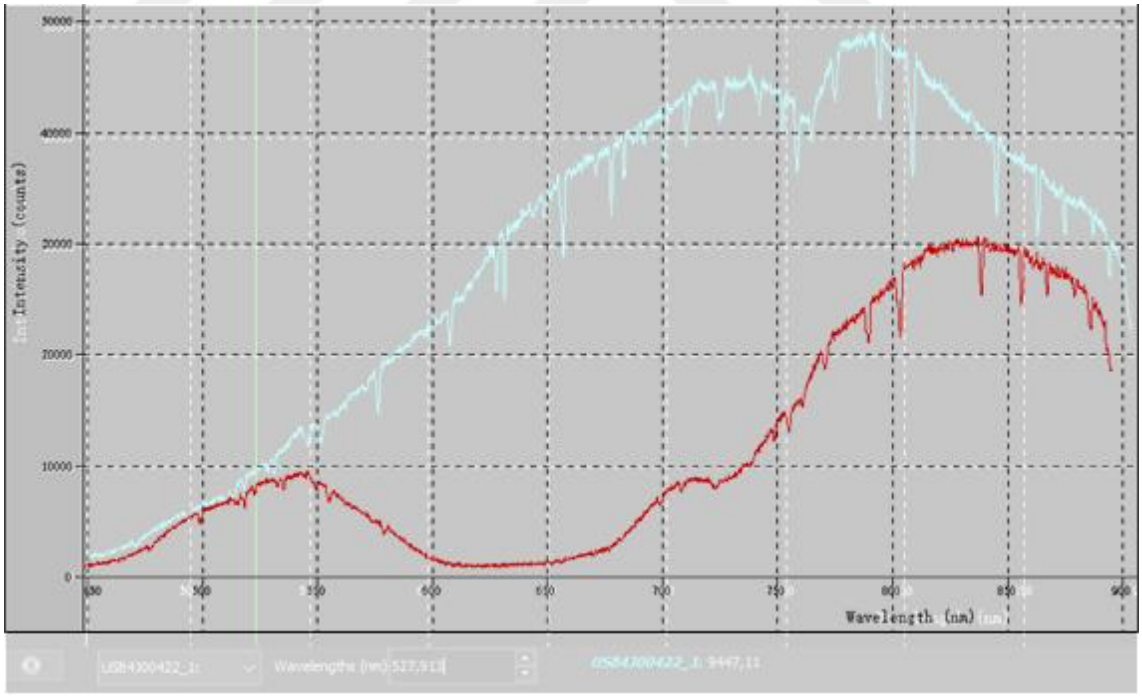

On the Figure 4.13, the cyan colored signal is the spectral response graph of the light bulb Phillips 9006 and the red colored signal is the actual blue and green acetates measurement.

Two green acetate films are tested and optical attenuation is obtained between 550-900 nm wavelength band. A total attenuation is observed between 600-675 nm wavelength band.

Figure 4.14: Two Green Acetate Films

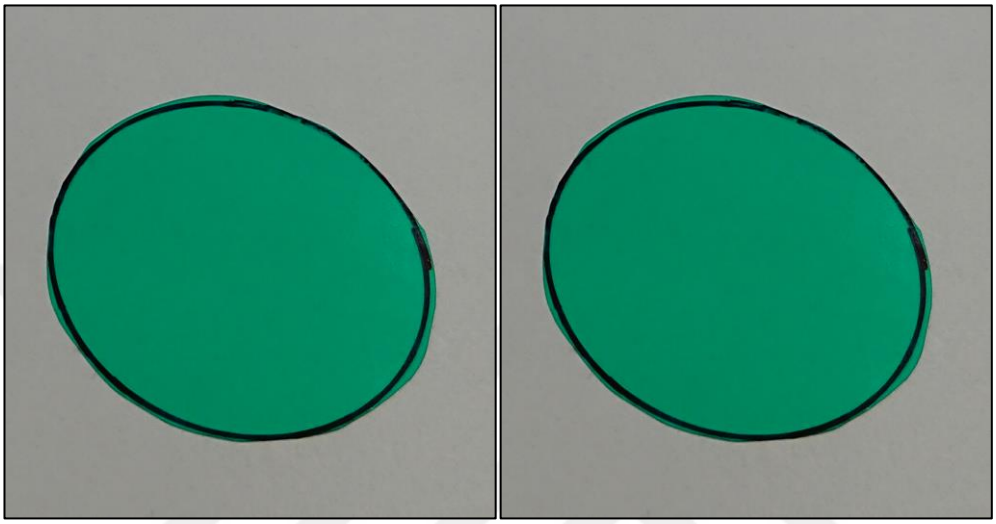

Figure 4.15: Spectral Graph of Two Green Acetate Films

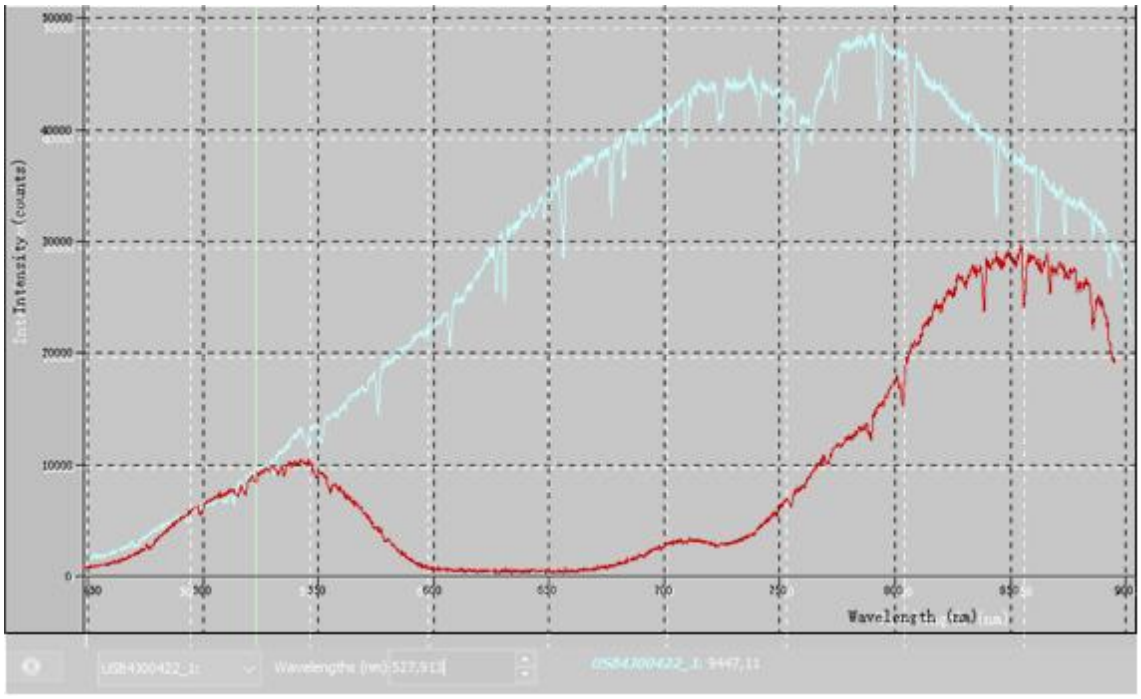

On the Figure 4.15, the cyan colored signal is the spectral response graph of the light bulb Phillips 9006 and the red colored signal is the actual two green acetates measurement. Two blue acetate films are tested and optical attenuation is obtained between 550-750 nm wavelength band. The efficiency was not as clear as green acetate.

Figure 4.16: Two Blue Acetate Films

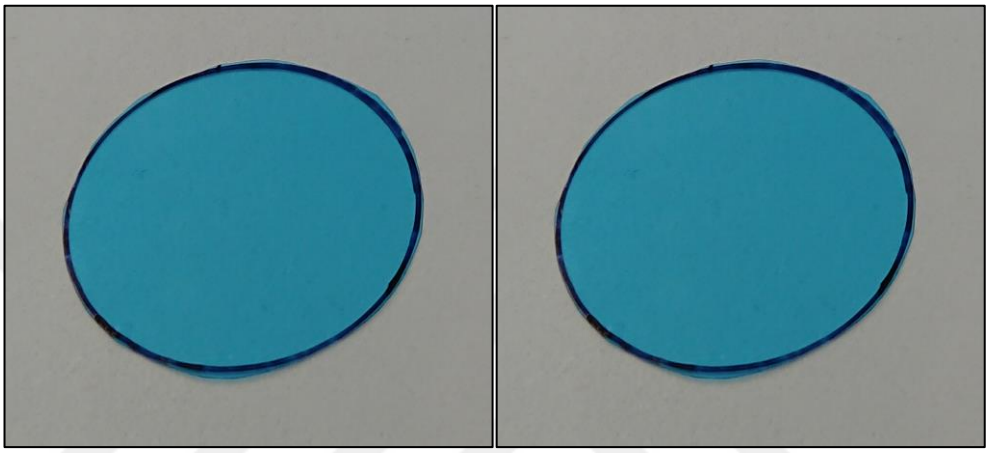

Figure 4.17: Spectral Graph of Two Blue Acetate Films

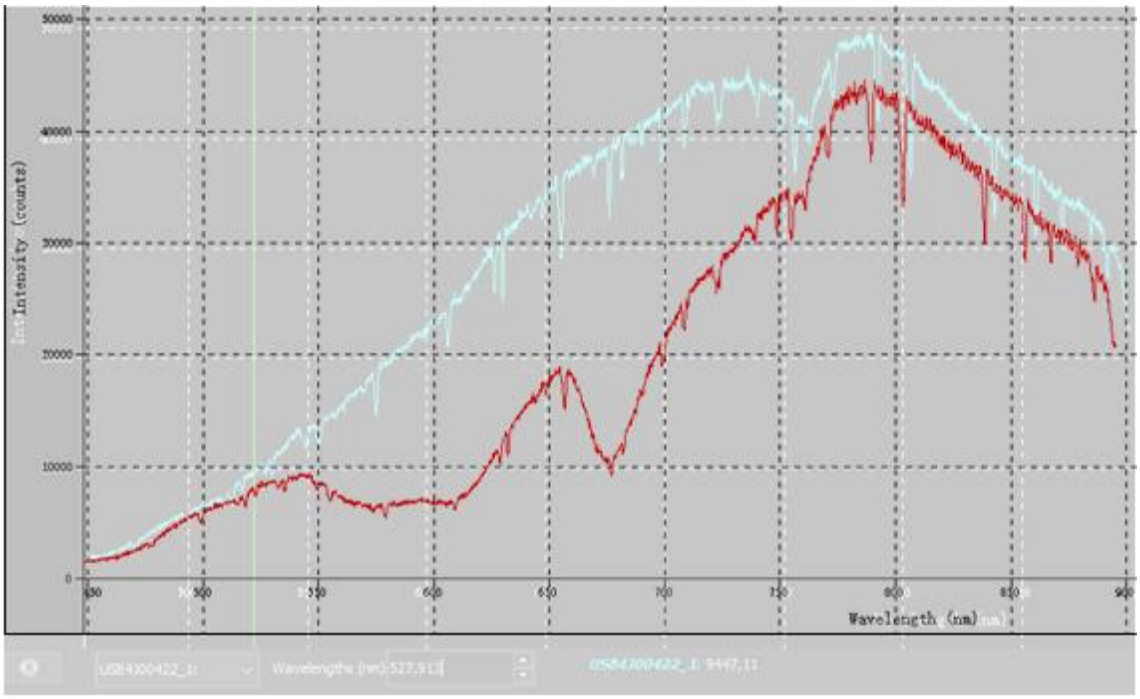

On the Figure 4.17 the cyan colored signal is the spectral response graph of the light bulb Phillips 9006 and the red colored signal is the actual two blue acetates measurement.

Two blue and two green acetate films are tested and optical attenuation is obtained between 550-900 nm wavelength band. A total attenuation is observed between 600-725 nm wavelength band.

Figure 4.18: Two Blue and Two Green Acetate Films

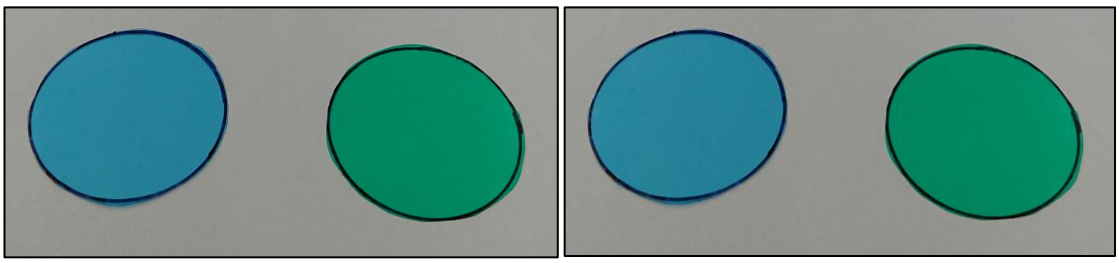

Figure 4.19: Spectral Graph of Two Blue and Two Green Acetate Films

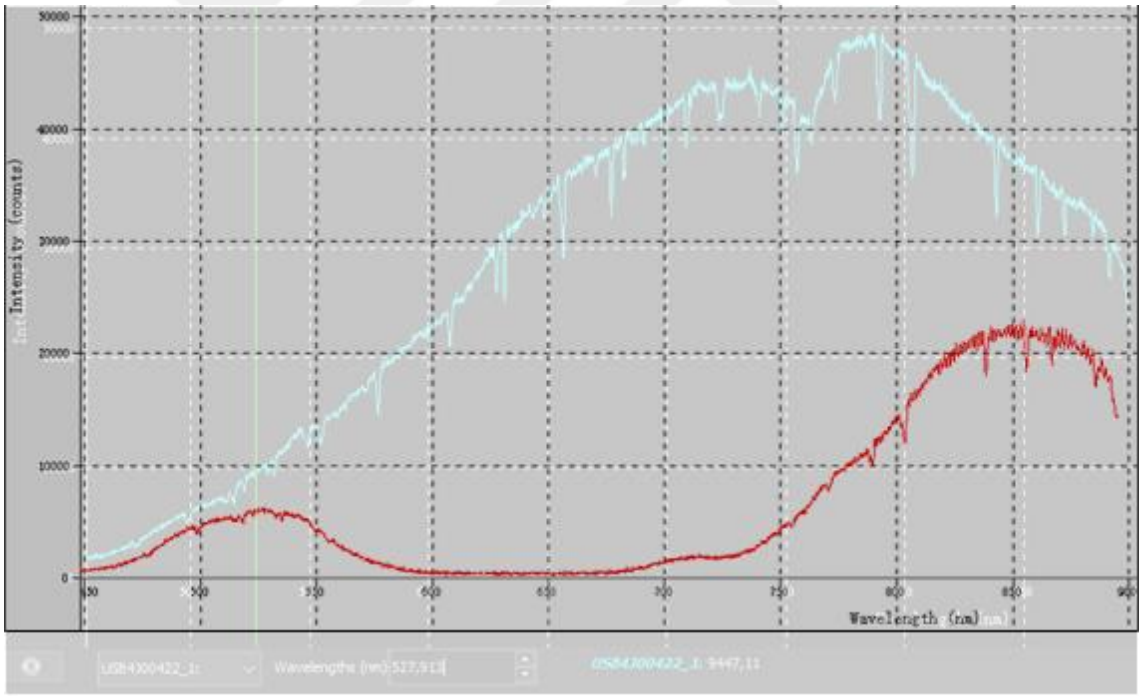

On the Figure 4.19, the cyan colored signal is the spectral response graph of the light bulb Phillips 9006 and the red colored signal is the actual two blue and two green acetates measurement.

Figure 4.20: Spectral Graph and Values of Chosen Filter Combination.

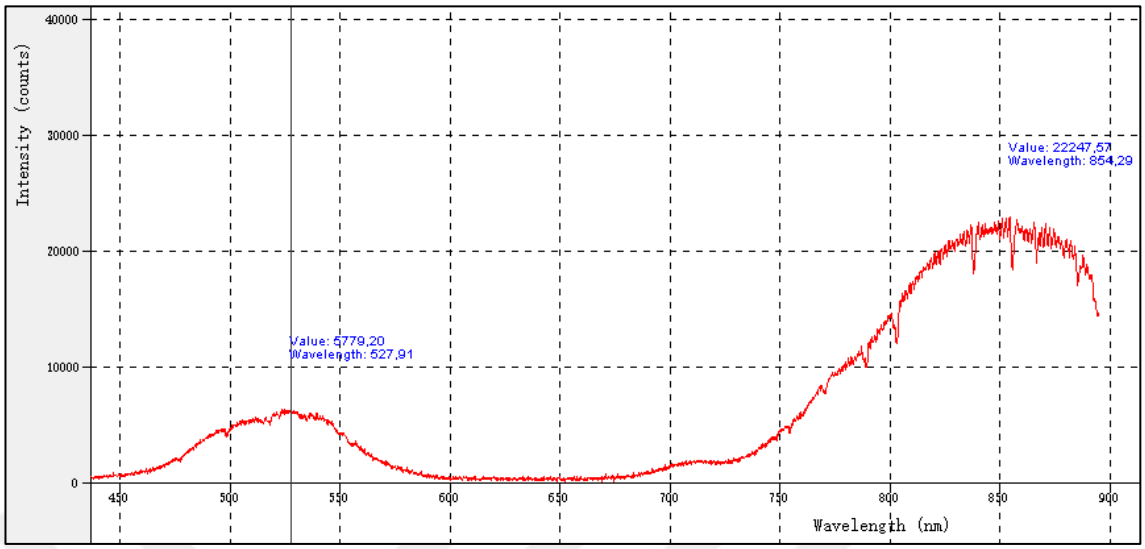

The infrared wavelength, 750-900 nm band, was still showing its effect. However an IR filter is not needed because, IR wavelengths are highly attenuated underwater environment. The filter combination of two blue and two green acetate films were selected to be used in the system.

4.4 Transmitter Test

The transmitter unit is needed to be tested for input sound signal acquisition, carrier frequency and modulation. Measurements are made with Bitscope Micro Oscilloscope and Analyzer. 1 kHz reference sound is generated with a mobile phone. The signal measurement is made from “Signal In” point on Figure 3.11. 1 kHz signal is measured and it is shown on Figure 4.21.

Figure 4.21: Sound signal frequency on oscilloscope

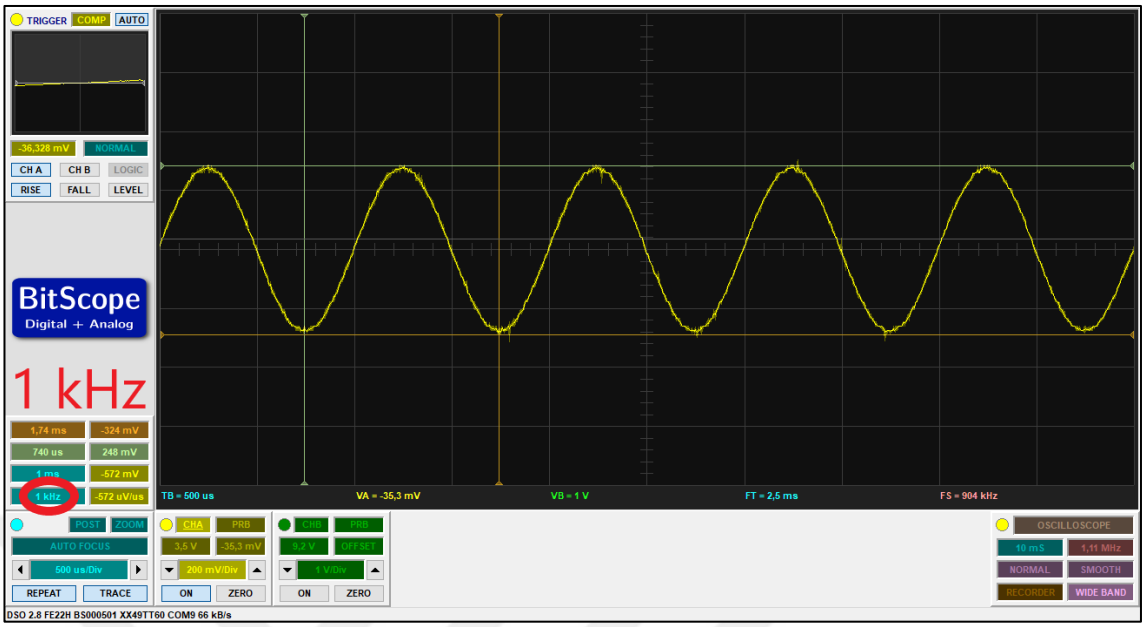

The carrier frequency is selected 62,5 kHz and it is mentioned on section 3.2.2. The signal measurement is made from "PWM Out" point on Figure 3.11. 62,5 kHz signal is measured and it is shown on Figure 4.22. The measurement is made while the reference signal 1 kHz was OFF to see the naked carrier frequency.

Figure 4.22: Carrier Frequency on oscilloscope

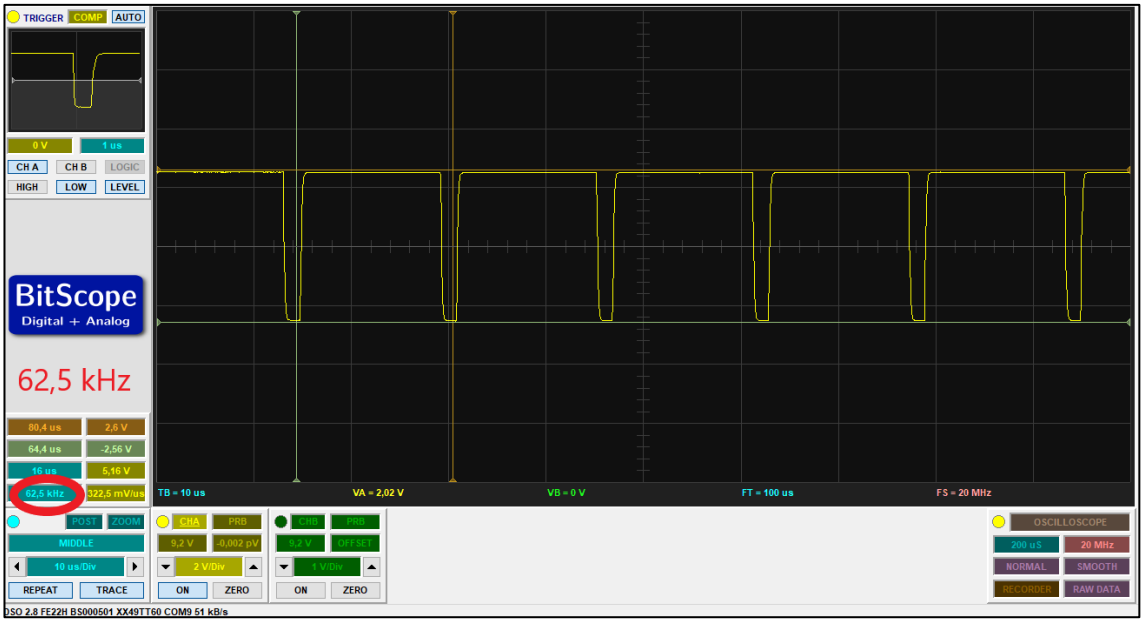

After the naked carrier frequency is seen, 1 kHz reference signal is given to circuit. The signal measurement is made from “PFM Out” point on Figure 3.11. PFM like PWM modulation is seen on Figure 4.23. The modulation signal shape was like desired shape and it is mentioned on section 3.2.2.

Figure 4.23: PFM like PWM Modulation

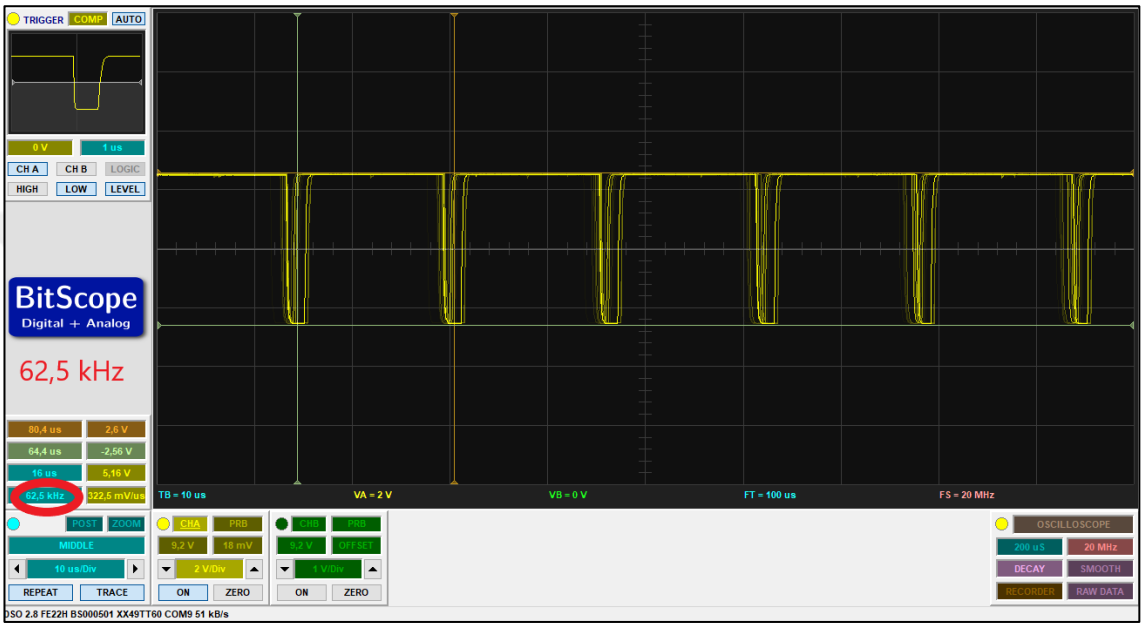

The final transmitter test was to check the LED state. LED state was ON and it shows the modulation is going and it is shown on Figure 4.23.

Figure 4.24: One transmitter and one receiver unit performing the communication.

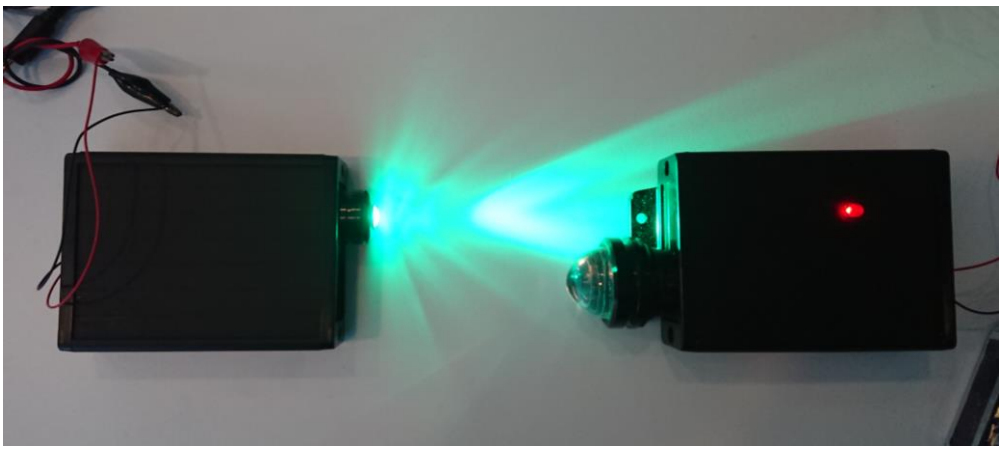

4.5 Receiver Test

The receiver unit is needed to be tested also for photodiode transimpedance amplifier output, signal conditioning LF356 output, demodulator LMC568 output and sound amplifier LM386 output. Measurements are made with Bitscope Micro Oscilloscope and Analyzer.

The signal measurement is made from OPA381 output pin “P6” on Figure 3.22. Modulated signal successfully acquired with emitted carrier frequency of 62,5 kHz and it is shown on Figure 4.25.

Figure 4.25: Transimpedance Amplifier Output

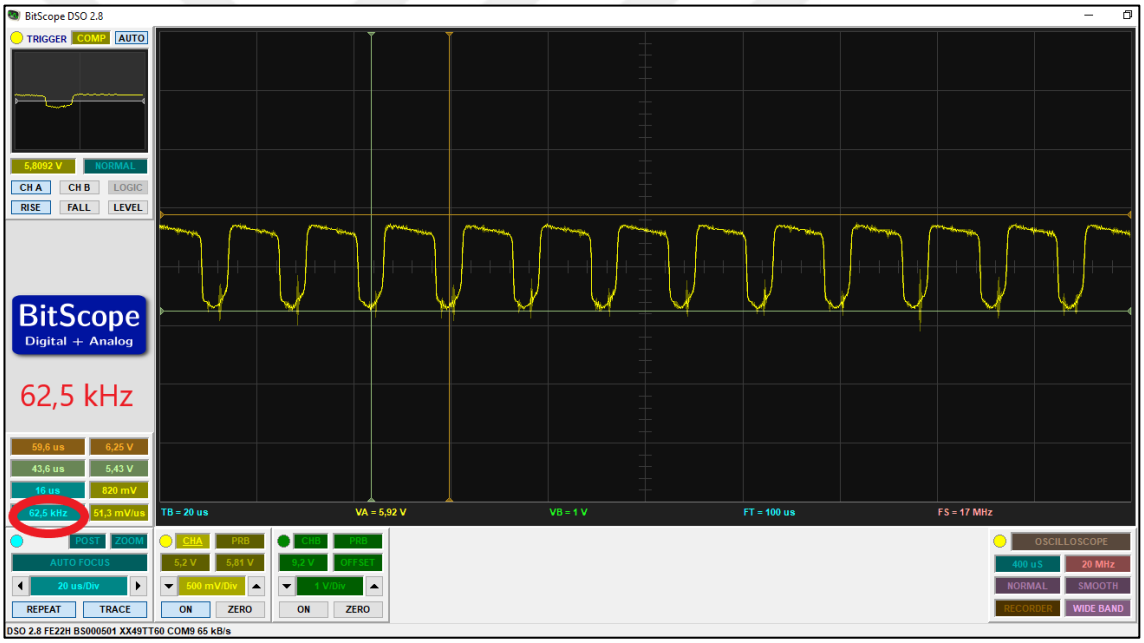

The signal conditioning of LF356 measurement is made from LF356 output pin on Figure 3.22. The received modulated signal amplified with 1V gain and it is shown on Figure 4.26 and the signal was being ready for demodulation process.

Figure 4.26: Lf356 Output

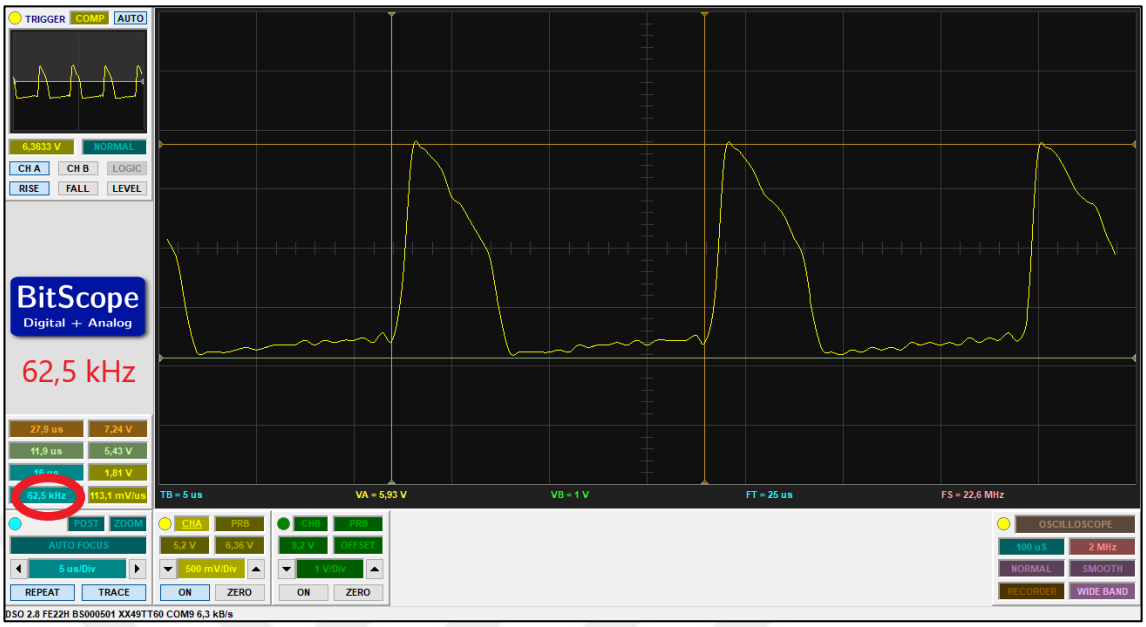

The demodulation of the modulated signal is made on LMC568 and the measurement is made from LMC568 output pin “P6” on Figure 3.22. The demodulated signal is shown on Figure 4.27. The demodulated signal is needed to be amplified to obtain the sound signal. It is also seen the reference 1 kHz signal on the Figure 4.27.

Figure 4.27: LMC568 Output

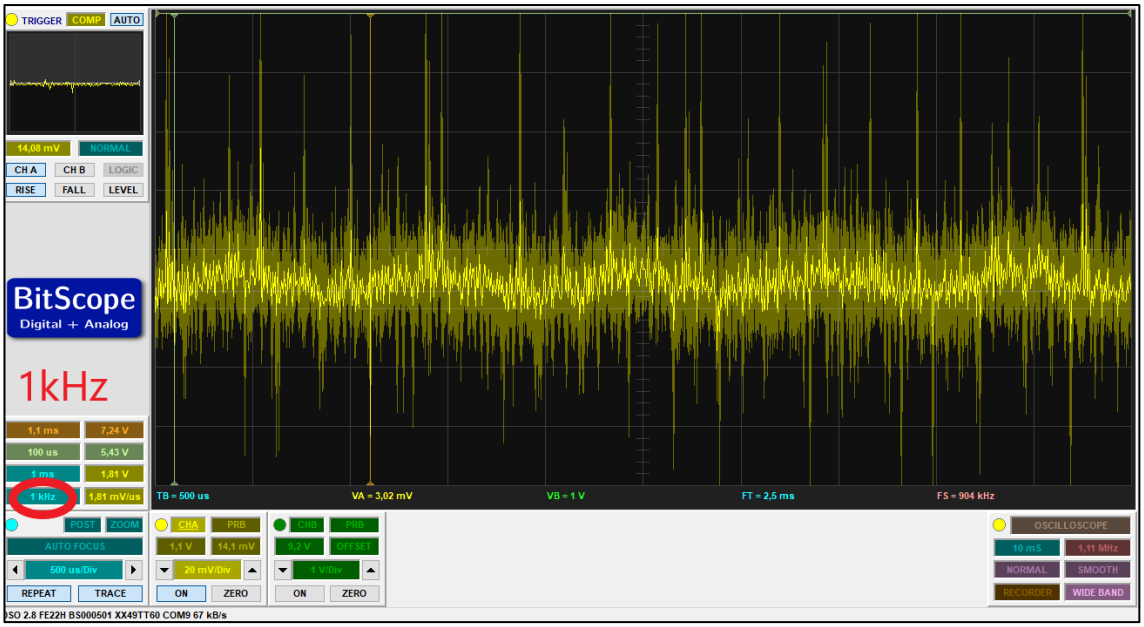

The demodulated signal is needed to be amplified to obtain pure 1 kHz signal. A low power audio amplifier LM386 is used to amplify the audio signal output. The measurement of Figure 4.28 is made from LM368 output pin “P8” on Figure 3.25.

Figure 4.28: LM386 Output

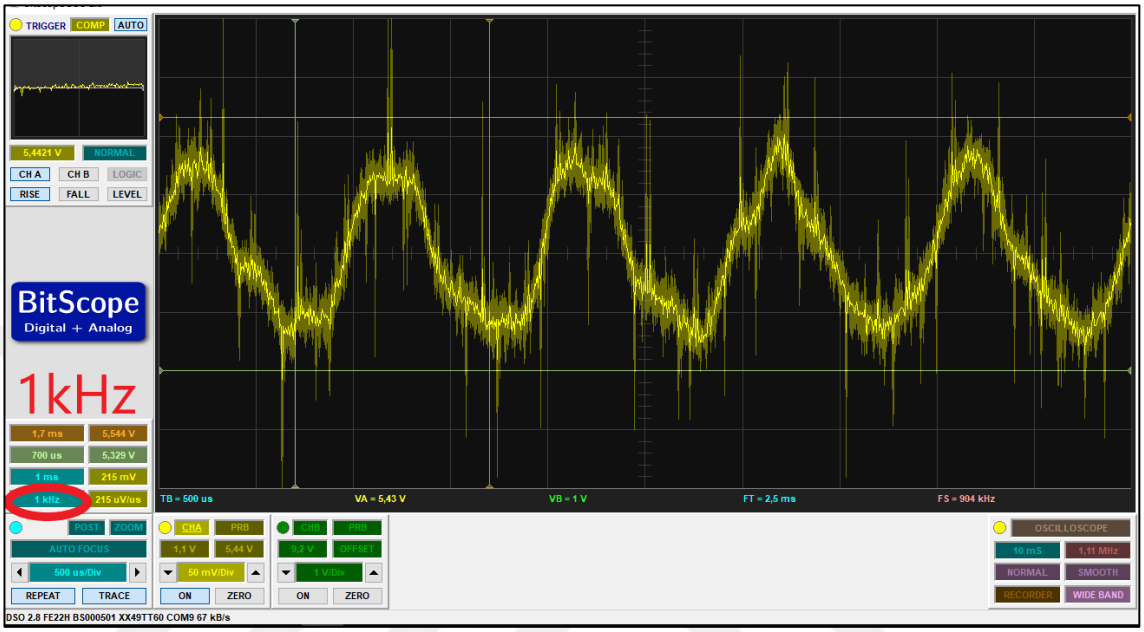

5. DISCUSSION

In this section, the real life applications of the proposed system will be discussed. An optical underwater communication system was built and field tested by our research group supported by the (Savunma Sanayi Müsteşarlığı) Undersecretariat of Defence Industry of Turkish Republic. Due to the classified nature of this project and its outcome, certain information will not be revealed. The project's aim was to realize an optical communication between an underwater platform and an airborne platform while the underwater platform was submerged. On Figure 5.1 and Figure 5.2 The system is tested on the field and a succesfull optical two-way communication is performed with a total distance of around 60 meters between the underwater and airborne units, (22 meters underwater and 38 meters in the air). The test is also made by comparing a verbally transmitted random letter sequence by received letter sequence between two operators. The two-way communication has been accomplished with no errors. The maximum distance is limited by the test area's sea depth and the crane bome length. One free space optical communication and one fully submersible underwater optical communication unit that has 99 transmitter unit of above work with the same specifications are shown respectively. The unit for the underwater platform was designed, produced and tested for underwater conditions.

Figure 5.1: The underwater optical communication unit (left) and the free space optical communication unit (right) of the two-way optical communication system.

The system is tested on the field and a succesfull optical two-way communication is performed with a total distance of around 60 meters between the underwater and airborne units, (22 meters underwater and 38 meters in the air). The test is also made by comparing a verbally transmitted random letter sequence by received letter sequence between two operators. The two-way communication has been accomplished with no errors. The maximum distance is limited by the test area's sea depth and the crane bome length.

Figure 5.2: Underwater optical communication unit is placed on the sea floor and the free space optical communication unit is placed at the top of the crane.

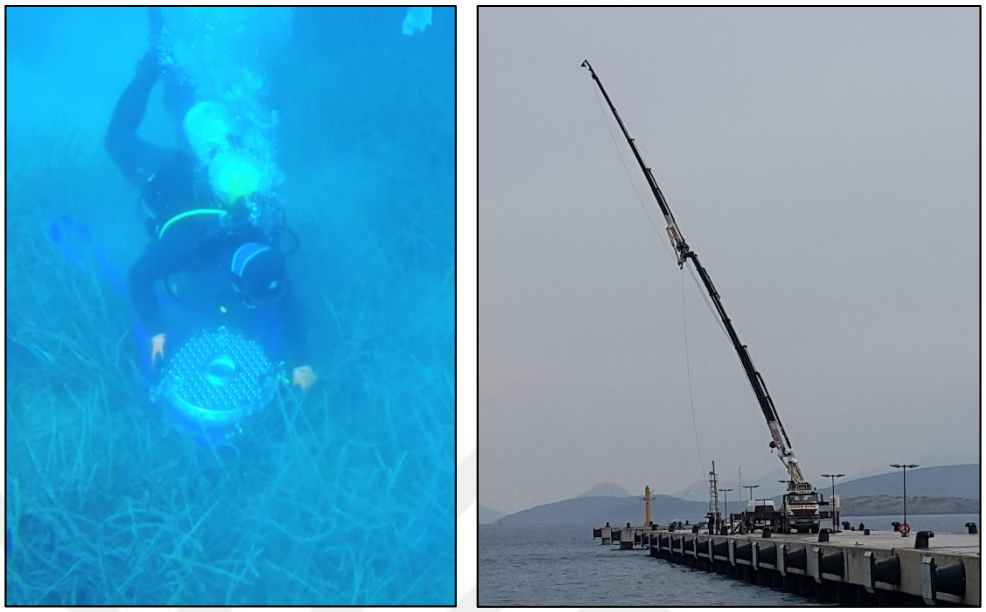

The concept of the constructed system is looks similar to class-D audio amplifiers. Class-D amplifiers are a switching amplifier, so called PWM amplifier. It has a PWM like waveform and the modulation frequency is higher than the human hearing range (approximately between 50 kHz to 250 kHz). The transmitted analog signal is modulated between human hearing range (20 Hz to 20 kHz), and since the processing unit is not a computer nor a digital system, human brain can recognize the transmitted voice signal just by resonance frequencies of the modulated signal. The circuits and all modulation types are analog; hence the only difficulty is to obtain a noise free signal. The next version of this prototype is desired to be digital and it is discussed in the next section Future Works.

6. CONCLUSION

The goal of this thesis was to present a new method to underwater optical voice communication by creating and implementing a prototype module based on LEDs that can transmit voice via light to be able to cope with some obstacles introduced by available data transmission techniques such as acoustics, electromagnetics etc.

The study has oriented majorly on building an underwater optical communication system that utilizes 505nm cyan color LED lights to transmit analog audio signals in full-duplex mode. Research prototypes are built and tested in laboratory condition with a distance of 15 meters and expected results were achieved as it was foreseen in the hypotheses of this study.

Beyond the laboratory tests, the performance of the system was tested in the real application field and very satisfactory results were obtained at around 60 meters part of which was under the water with a system having 99 LEDs installed.

6.1 FUTURE WORKS

This study is performed with all analog systems nevertheless, to make it more industry applicable and also to increase the application variety and to add more technical features such as noise cancelation, data encryption, channel modeling and so forth, it is highly recommended to build the system digitally.

The digital system can be built by using various digital elements such as advanced computer CPUs, microcontroller (MCUs), and digital audio chips but it is highly recommended to build it with FPGA above all. There are highly capable chipsets in the industry to comply the future applications of this system. One suggestion is to use Cypress PSoC 6 32-bit ARM CPU integrated with FPGA that may also add internet connectivity to the future devices.

Another suggestion would be to work on optical side of the system. One progress could be on lens development and increment of the distance with same power. Another

improvement could be to test color changing and trying to improve the transmission distance and data quality. If it is integrated with a fully digital system, then correct delivery of the digital data would be expected with different light color (i.e. bandwidth) and lens types.

Furthermore, the system may also include a feedback adjustment system for optical focusing as well as light color determination.

7. APPENDICES

7.1 Appendix A

```
f = 1e3:1e2:3.5e9;
c = physconst('LightSpeed') ./ 1.33;
sigmadw = .001; %conductivity of distilled water
sigmafw = .05;  %conductivity of fresh water
sigmasw = 4;    %conductivity of sea water
per_wtr = 0.9999912;
el_per_wtr = 81 .* 1e-10 ./ (36 .* pi);

p_spd_light (1 : length(f)) = c;
p_spd_sound (1 : length(f)) = 1500;
p_spd_rf_fw (1 : length(f)) = 1 ./ sqrt(per_wtr .* el_per_wtr);
p_spd_rf_sw = [];
for i = 1 : length(f)
    p_spd_rf_sw (i) = sqrt((4 .* pi .* f(i)) ./ ( per_wtr .* sigmasw));
end
figure
    semilogy(f,p_spd_light);hold on;
    semilogy(f,p_spd_sound);hold on;
    semilogy(f,p_spd_rf_fw);hold on;
    semilogy(f,p_spd_rf_sw);

        grid on;
        xlim auto
        ylim auto
legend('light', 'acoustic', 'Fresh Wtr','Sea Water')
xlabel('Frequency (Hz)');
ylabel('Propagation Speed (m/s)');
```

7.2 Appendix B

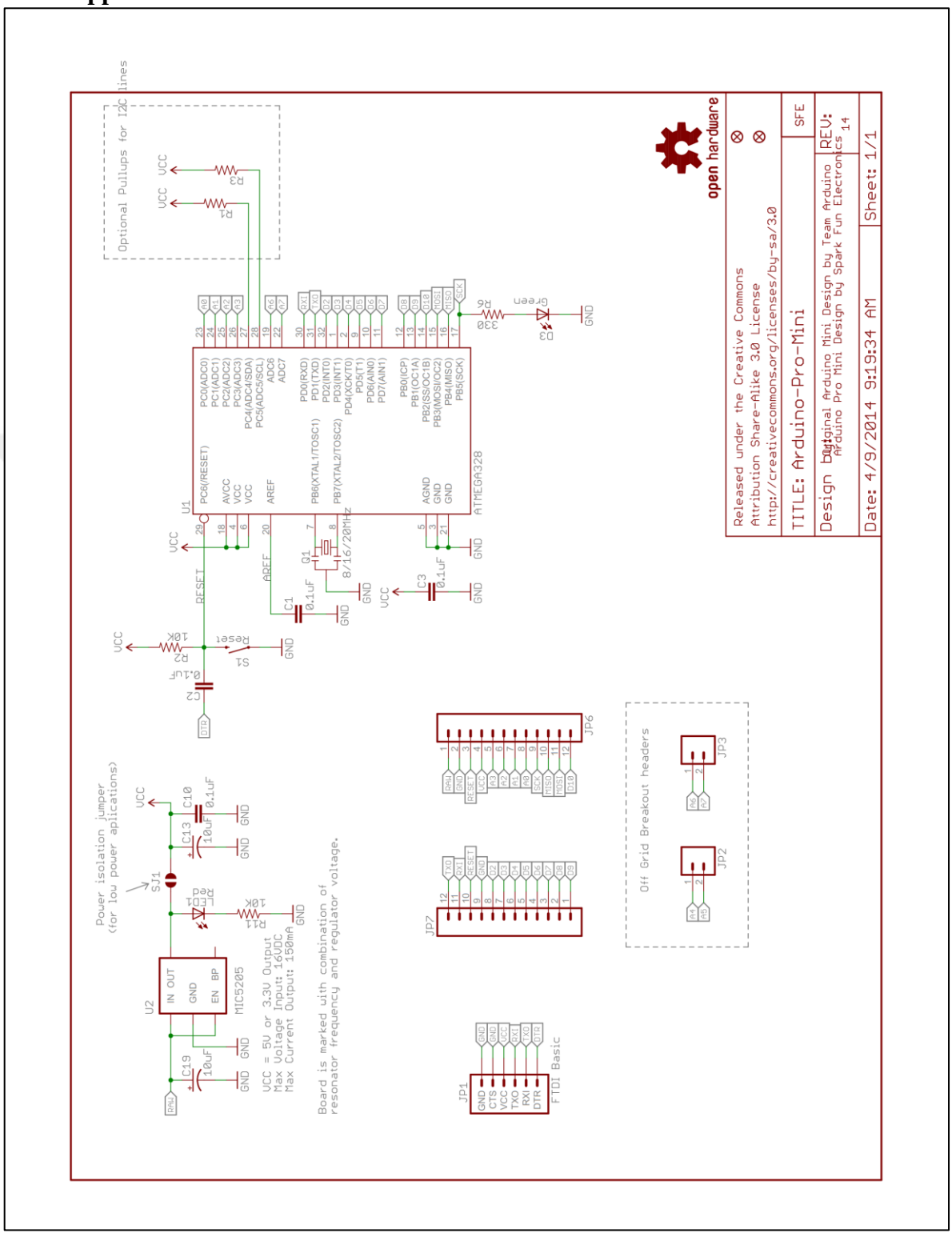

7.3 Appendix C

```
// Analog Audio Signal Input to PWM converter
// Referred from openmusiclabs.com version 1.9.13
// options table is taken from http://wiki.openmusiclabs.com/wiki/PWMDAC
// this code is simply, takes an audio data input from the Atmge328 ADC ports and plays it out on
// Timer1 PWM.  16b, Fast Mode PWM, 62,5 kHz - although ADC is 10bit.

#define PWM_FREQ 0x00FF // pwm frequency - see table
#define PWM_MODE 1 // adjust the Fast (1) Phase Correct (0)
#define PWM_QTY 2 // number of pwms, either 1 or 2

void setup() {// the setup of ADC input
  ADMUX = 0x60; // chooses the adc0 port
  ADCSRA = 0xe5; // turn on the adc ports with ck/32 and auto trigger
  ADCSRB =0x07; // timer 1 capture for trigger
  DIDR0 = 0x01; // turn off the digital inputs for adc0 port

  // setup of the PWM output
  TCCR1A = (((PWM_QTY - 1) << 5) | 0x80 | (PWM_MODE << 1)); //
  TCCR1B = ((PWM_MODE << 3) | 0x11); // ck/1
  TIMSK1 = 0x20; // assign the interrupt on capture mode
  ICR1H = (PWM_FREQ >> 8);
  ICR1L = (PWM_FREQ & 0xff);
  DDRB |= ((PWM_QTY << 1) | 0x02); // turn on the output ports

  sei(); // turn on interrupt cycle
}

void loop() {
  while(1); // run the code in infinite loop
}

ISR(TIMER1_CAPT_vect) {

 // gets ADC data
  unsigned int temp1 = ADCL;
  unsigned int temp2 = ADCH;
 // output the high byte on OC1A port
  OCR1AH = temp2 >> 8; // takes top 8 bits
  OCR1AL = temp2; // takes bottom 8 bits
// output the low byte on OC1B port
  OCR1BH = temp1 >> 8;
  OCR1BL = temp1;
}
```

7.4 Appendix D

```
d = 0.1:0.1:100;
Iin = 656.3; %70 lumens in 0.01 meter
Kd = 0.04679;  %diffuse attenuation coefficient in 488nm
 for i = 1 : length(d)
    Idis (i) = Iin .* exp(-Kd.*d(i));
end
figure
    plot(d,Idis);
        grid on;
       xlim auto
       ylim auto
        xlabel('distance (m)');
ylabel('light intensity (Lux)');
```

8. References

Books

AUSTION, R. W. & PETZOLD, T. J. 1981. The Determination of the Diffuse Attenuation Coefficient of Sea Water Using the Coastal Zone Color Scanner. *Oceanography from Space.* Boston, MA: Springer.

BEECH, M. 2012. The physics of invisibility a story of light and deception. New York, NY: Springer,.

BELEFFI, G. M. T. 2010. Free Space Optical Technologies. *In:* BOURAS, C. J. (ed.) *Trends in Telecommunications Technologies.*

BENVENUTO, N., ZORZI, M. & WILEY INTERSCIENCE (ONLINE SERVICE) 2011. Principles of communications networks and systems. Chichester: Wiley,.

GAY-LUSSAC, M. & ARAGO, M. 1827. *Annales de Chimie et de Physique,* Paris.

GHASSEMLOOY, Z., POPOOLA, W. & RAJBHANDARI, S. 2013. Optical wireless communications system and channel modelling with MATLAB. Boca Raton, FL: CRC Press,.

GUYTON, A. C. & HALL, J. E. 2006. *Textbook of Medical Physiology*, Elsevier Saunders.

HOLT, A., HUANG, C.-Y. & SPRINGERLINK (ONLINE SERVICE) 2010. 802.11 wireless networks security and analysis. *Computer communications and networks.* London: Springer,.

HOSPITALIER, É. 1882. *Les principales applications de l'électricité,* Paris, G. Masson.

JERLOV, N. G. 1976. *Marine optics,* Amsterdam ; New York, Elsevier Scientific Pub. Co.

KOUPELIS, T. 2011. *In quest of the universe,* Sudbury, Mass., Jones and Bartlett Publishers.

LANZAGORTA, M. 2013. Underwater communications. *Synthesis lectures on communications,.* San Rafael, Calif. (1537 Fourth Street, San Rafael, CA 94901 USA): Morgan & Claypool,.

LURTON, X. 2002. *An introduction to underwater acoustics : principles and applications,* London ; New York Chichester, UK, Springer ; Published in association with Praxis Pub.

MEDWIN, H. & CLAY, C. S. 1998. *Fundamentals of acoustical oceanography,* Boston, Academic Press.

MOBLEY, C. D. 1994. *Light and water : radiative transfer in natural waters,* San Diego, Academic Press.

RSTC 2005. Minimum Course Content for Common Hand Signals for Scuba Diving. Florida, USA: Recreational Scuba Traning Council, Inc.

SPINRAD, R. W., CARDER, K. L. & PERRY, M. J. 1994. *Ocean optics,* New York ; Oxford, Oxford University Press.

UYSAL, M., CAPSONI, C., GHASSEMLOOY, Z., BOUCOUVALAS, A. C. & UDVARY, E. 2016. Optical wireless communications : an emerging technology. *Signals and communication technology,.* Switzerland: Springer,.

WAITE, A. D. 2002. *Sonar for practising engineers,* Chichester, Wiley.

Journal Articles

COCHENOUR, B. M., MULLEN, L. J. & LAUX, A. E. 2008. Characterization of the Beam-Spread Function for Underwater Wireless Optical Communications Links. *IEEE Journal of Oceanic Engineering,* 33**,** 513-521.

DUNTLEY, S. Q. 1963. Light in the Sea. *Journal of the Optical Society of Ameria,* 53**,** 214-233.

GILBERT, G. D., STONER, T. R. & JERNIGAN, J. L. 1966. Underwater Experiments On The Polarization, Coherence, And Scattering Properties Of A Pulsed Blue-Green Laser. *Proc. SPIE,* 7**,** AII1-7.

HALTRIN, V. I. 1999. Chlorophyll-based model of seawater optical properties. *Applied Optics,* 38**,** 6826-6832.

JOHNSON, L. J., GREEN, R. J. & LEESON, M. S. 2013. Underwater optical wireless comunications: depth dependent variations in attenuation. *Applied Optics,* 52**,** 7867-7873.

JOHNSON, L. J., JASMAN, F., GREEN, R. J. & LEESON, M. S. 2014. Recent advances in underwater optical wireless communications. *Society of Underwater Technology,* 32**,** 167-175.
KATZIR, S. 2012. Who knew piezoelectricty? Rutherford and Langevin on submarine detection and the invention of sonar. *Notes & Records of the Royal Society,* 66**,** 141-157.
LINDSAY, J. B. 1854. Further Experiments of Mr. Lindsay's New Patent Trans-Marine Telegraph. *The Dundee Courier*.
LIU, L., ZHOU, S. & CUI, J.-H. 2008. Prospects and problems of wireless communication for underwater sensor networks. *Wireless Communications and Mobile Computing,* 8**,** 977-994.
PENG, C., ZHAO, X. & LIU, G. 2015. Noise in the Sea and Its Impacts on Marine Organisms. *Int J Environ Res Public Health,* 12**,** 12304-23.
QUAZI, A. & KONRAD, W. 1982. Underwater Acoustic Communications. *IEEE Communications Magazine,* 20**,** 24-30.
SIEGEL, M. & KING, R. 1973. Electromagnetic propagation between antennas submerged in the ocean. *IEEE Transactions on Antennas and Proagation,* 21**,** 507-713.
TILTON, L. W. & TAYLOR, J. K. 1938. Refractive index and dispersion of distilled water for visible radiation, at temperature 0 to 60 C. *Journal of Research of the National Bureau of Standars,* 20**,** 419-477.

Web Pages

WIKIHOW. 2017. *wikiHow to Communicate Underwater when Scuba Diving* [Online]. Available: https://www.wikihow.com/Communicate-Underwater-when-Scuba-Diving [Accessed].

Reports

E. J. HILLIARD, J. & GOULD, G. G. 1977. Electromagnetic Radiation in Sea Water. Newport, Rhode Island: U. S. Naval Underwater Ordanance Station.
U.S.NAVY 2003. Extremely Low Frequency Transmitter Site Clam Lake, Wisconsin.

Magazine Article

BUTLER, L. 1987. Underwater Radio Communication. *Amateur Radio.* Melbourne: Wireless Institute of Australia.

Newspaper Article

LINDSAY, J. B. 1853. Mr Lindsay's Marine Telegraph. *Dundee, Perth and Cupar Advertiser*.
LINDSAY, J. B. 1860. Transmarine Telegrapg. *The South Australian Advertiser*.

Catalogs

OCEANREEF 2010. Underwater Communication: Skills for a new way of diving. *In:* GROUP, O. (ed.). California, USA: Oceanreef Group.

Uncategorized References

BAZEILLE, S., QUIDU, I. & JAULIN, L. 2012. Color-based underwater object recognition using water light attenuation. *Intelligent Service Robotics,* 5**,** 109-118.
LEE, Z.-P., DARECKI, M., CARDER, K., L., DAVIS, C. O., STAMSKI, D. & RHEA, W. J. 2005. Diffuse attenuation coefficient of downwelling irradiance: An evaluation of remote sensing methods. *Journal of Geophysical Research,* 110**,** 1-9.
STAIR, R. G., RUSSELL; BAGG, THOMAS C. 1954. Spectral Distribution of Energy From the Sun. *Journal of Research of the National Bureau of Standars,* 53**,** 113-119.